Mechanistic and Structural Features of PROTAC Ternary Complexes

Casement, Ryan; Bond, Adam; Craigon, Conner; Ciulli, Alessio

Published in:
Targeted Protein Degradation

DOI:
10.1007/978-1-0716-1665-9_5

Publication date:
2021

Document Version
Peer reviewed version

Casement, Ryan et al. "Mechanistic and Structural Features of PROTAC Ternary Complexes"., Cacace, Angela M. Hickey, Christopher M. Békés, Miklós (editors). Targeted Protein Degradation: Methods and Protocols. 1 udg., Methods in Molecular Biology. New York: Humana Press. 2021, 79-113. https://doi.org/10.1007/978-1-0716-1665-9_5

Metadata of the chapter that will be visualized online

Chapter Title	Mechanistic and Structural Features of PROTAC Ternary Complexes	
Copyright Year	2021	
Copyright Holder	Springer Science+Business Media, LLC, part of Springer Nature	
Author	Family Name	**Casement**
	Particle	
	Given Name	**Ryan**
	Suffix	
	Division	Division of Biological Chemistry and Drug Discovery, School of Life Sciences
	Organization	University of Dundee
	Address	Dundee, Scotland, UK
Author	Family Name	**Bond**
	Particle	
	Given Name	**Adam**
	Suffix	
	Division	Division of Biological Chemistry and Drug Discovery, School of Life Sciences
	Organization	University of Dundee
	Address	Dundee, Scotland, UK
Author	Family Name	**Craigon**
	Particle	
	Given Name	**Conner**
	Suffix	
	Division	Division of Biological Chemistry and Drug Discovery, School of Life Sciences
	Organization	University of Dundee
	Address	Dundee, Scotland, UK
Corresponding Author	Family Name	**Ciulli**
	Particle	
	Given Name	**Alessio**
	Suffix	
	Division	Division of Biological Chemistry and Drug Discovery, School of Life Sciences
	Organization	University of Dundee
	Address	Dundee, Scotland, UK
	Email	a.ciulli@dundee.ac.uk
Abstract	The rapid and ever-growing advancements from within the field of proteolysis-targeting chimeras (PROTAC)-induced protein degradation	

have driven considerable development to gain a deeper understanding of their mode of action. The ternary complex formed by PROTACs with their target protein and E3 ubiquitin ligase is the key species in their substoichiometric catalytic mechanism. Here, we describe the theoretical framework that underpins ternary complexes, including a current understanding of the three-component binding model, cooperativity, hook effect and structural considerations. We discuss in detail the biophysical methods used to interrogate ternary complex formation in vitro, including X-ray crystallography, AlphaLISA, FRET, FP, ITC and SPR. Finally, we provide detailed ITC methods and discuss approaches to assess binary and ternary target engagement, target ubiquitination and degradation that can be used to obtain a more holistic understanding of the mode of action within a cellular environment.

Keywords (separated by '-')

Targeted protein degradation (TPD) - proteolysis-targeting chimeras (PROTACs) - E3 ubiquitin ligase - Ternary complex - Hook effect - Cooperativity - Biophysical methods, crystal structures - Target engagement - Protein ubiquitination

Chapter 5

Mechanistic and Structural Features of PROTAC Ternary Complexes

Ryan Casement, Adam Bond, Conner Craigon, and Alessio Ciulli

Abstract

The rapid and ever-growing advancements from within the field of proteolysis-targeting chimeras (PROTAC)-induced protein degradation have driven considerable development to gain a deeper understanding of their mode of action. The ternary complex formed by PROTACs with their target protein and E3 ubiquitin ligase is the key species in their substoichiometric catalytic mechanism. Here, we describe the theoretical framework that underpins ternary complexes, including a current understanding of the three-component binding model, cooperativity, hook effect and structural considerations. We discuss in detail the biophysical methods used to interrogate ternary complex formation in vitro, including X-ray crystallography, AlphaLISA, FRET, FP, ITC and SPR. Finally, we provide detailed ITC methods and discuss approaches to assess binary and ternary target engagement, target ubiquitination and degradation that can be used to obtain a more holistic understanding of the mode of action within a cellular environment.

Key words Targeted protein degradation (TPD), proteolysis-targeting chimeras (PROTACs), E3 ubiquitin ligase, Ternary complex, Hook effect, Cooperativity, Biophysical methods, crystal structures, Target engagement, Protein ubiquitination

1 PROTAC Ternary Complexes: Equilibria and Crystal Structures

1.1 Two-Component vs. Three-Component Binding Models

Two-body binding equilibria have classically been addressed by the Hill–Langmuir equation which was formulated by Archibald Hill in 1910 to describe the interaction of oxygen with haemoglobin [1]. Since then, the sigmoidal dose–response curve which describes these systems has become a permanent fixture in drug discovery for the evaluation of ligands interacting with proteins.

As new chemical biology modalities such as bispecific antibodies [2], bivalent inhibitors [3–5], molecular glues [6] and most recently proteolysis-targeting chimeras (PROTACs) [7] have come to the fore, there is now an increased need to understand three-

Ryan Casement, Adam Bond and Conner Craigon contributed equally to this work.

Angela M. Cacace, Christopher M. Hickey and Miklós Békés (eds.), *Targeted Protein Degradation: Methods and Protocols*, Methods in Molecular Biology, vol. 2365, https://doi.org/10.1007/978-1-0716-1665-9_5,

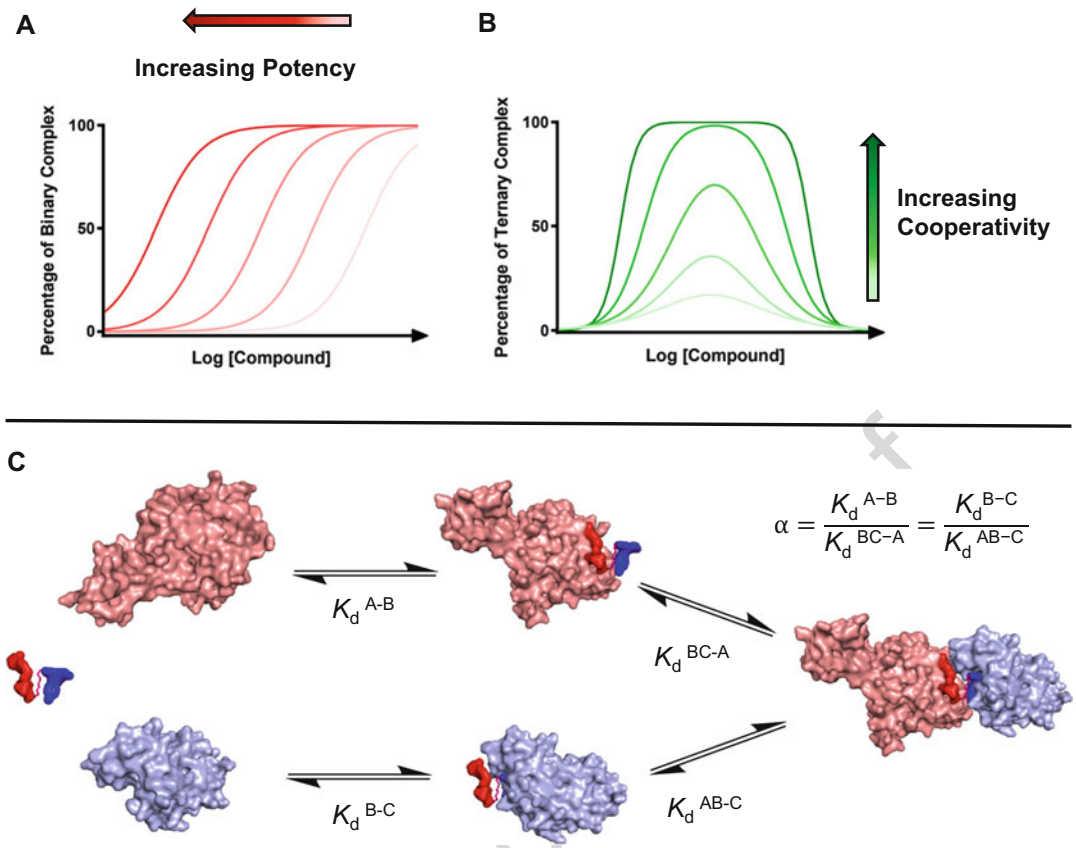

Fig. 1 Comparison of binary and ternary complex formation. (**a**) Simulated dose–response curves using the Hill–Langmuir equation where increasing potency results in a left shift of the sigmoidal dose–response curve. (**b**) Depiction of bell-shaped dose–response curves typical in ternary complex formation. Increased cooperativity of a system results in improved ternary complex formation and heightening and widening of the curve. (**c**) Depiction of potential binding cycle of PROTAC-induced ternary complexes adapted from PDB 5T35. PROTAC shown as a red and blue surface joined by a linker, the PROTAC can either bind protein 'A' (pink surface) or protein 'B' first and cooperativity (α) can be calculated from the K_d values from the individual steps

component binding models and the characteristics of the ternary complex formed (Fig. 1). Bivalent modalities can be visualised to form a ternary complex in a two-step process as depicted in Fig. 1c. In the case of PROTACs, the binding order here could potentially be random, while molecular glues such as immunomodulatory imine drugs (IMiDs) have been shown to require binding to a specific protein (Cereblon or CRBN) before neo-substrates can be recruited [8]. Unlike the classical sigmoidal curve which is used to describe many two-body systems (Fig. 1a), the binding isotherm describing the formation of ternary complexes is usually represented by a bell-shaped curve (Fig. 1b). The first half of the isotherm is visually similar to that of a binary system until the point of saturation after which increasing ligand concentration will eventually decrease ternary complex concentration, a phenomenon

commonly known as the hook effect [9]. In addition, a further layer of complexity is added by potential interactions between the two protein-binding partners, resulting in cooperativity effects which essentially delineates ternary and binary binding affinities and modulates the height and width of the curve [10].

1.2 Cooperativity and the Hook Effect

The hook effect describes the declining effectiveness of a bifunctional molecule in forming a ternary complex at high concentrations due to the preferential formation of multiple binary complexes. This effect was observed as early as 1905 when the presence of a bell-shaped curve in immunoprecipitation assays was said to be caused by the 'prozone phenomenon' [11]. As well as causing issues in immune assays, the hook effect essentially limits the therapeutic window of potential therapeutics. This 'dose-limited activity' has been shown in monoclonal antibody therapies which operate via antibody-dependent cell-mediated cytotoxicity (ADCC) [12]. PROTAC's hook effect was observed following western blotting, with the loss of protein degradation at high compound concentrations [13]. It was later observed biophysically, with the appearance of bell-shaped curves in the amplified luminescent proximity homogeneous assays (AlphaScreen or AlphaLISA) measuring ternary complex formation [14, 15]. One interesting observation is that not all PROTACs 'hook' equally potentially due to cooperativity effects as it has been shown that the hook effect can be attenuated by cooperativity [16].

PROTACs mode of action strictly depends on the formation of a ternary complex that is productive to subsequent target ubiquitination and degradation. This can be achieved in principle in a substoichiometric fashion (i.e. without the need to occupy in full the target protein) and via a catalytic cycle (i.e. the same molecule of PROTAC can deliver multiple cycles of protein ubiquitination and degradation). These features are predicted to drive potent target degradation activities at low PROTAC concentration and therefore in the first instance should correlate linearly with the amount of ternary complex. It is therefore important to better understand ternary complex formation equilibria and how they impact PROTAC mode of action (Fig. 1).

In the context of ternary complex formation, cooperativity (α) describes the increased affinity a ligand 'B' has for 'Protein A' in the presence of 'Protein C' vs. 'Protein A' alone. For PROTACs, A and C are usually different with one being an E3 ligase, but they could be the same species in the case of homo-PROTACs that dimerise an E3 ligase for self-degradation [17, 18]. Positive α values describe a cooperative system which favours the formation of the ternary complex and in the context of a bell-shaped curve (Fig. 1) essentially heightens and widens the curve, extending the activity range of any potential therapeutic. One prominent example of cooperativity from nature comes from bacterial superantigens. These are

bacterial toxins which exert their effect by binding major histocompatibility complex (MHC) class II molecules and T-cell receptors (TCR) to form a ternary complex, cross-linking T cells with antigen-presenting cells and resulting in a cytokine storm [19]. This interaction has been found be to be highly cooperative by surface plasmon resonance (SPR) [20].

Molecular glues by definition cause the formation of stable ternary complexes often overcoming weak binary binding affinities and as such rely heavily on cooperativity for their activity. Examples include natural products such as rapamycin and the plant hormone auxin which highlights the structural diversity of molecular glues [21, 22]. While the 31-membered macrocycle rapamycin has a molecular weight of 914 Da and a total of 15 stereocentres, auxin (Indole-3-acetic acid) has a molecular weight of only 175 Da. Rapamycin which is approved as an immunosuppressant for organ transplant patients forms a ternary complex with FK506 binding protein (FKBP) and the FRB binding domain of the molecular target of rapamycin (mTOR) resulting in potent mTOR inhibition [21]. In a thorough biophysical characterisation of this complex, it was found that rapamycin binds to FRB with a 2000-fold improved binding affinity in the presence of FKBP [23]. Auxin functions as a plant hormone via binding to TIR1 and the subsequent recruitment of neo-substrates such as members of the Aux/IAA protein family. As TIR1 is the substrate receptor of a SCF E3 ligase, this interaction results in the proteasomal degradation of Aux/IAAs and effectively activates transcription of auxin response factor (ARF) proteins [22].

In addition to natural products, there are examples of synthetic molecular glues such as Indisulam and Thalidomide which were developed before their gluing activity was fully understood. These therapeutics recruit neo-substrates to the E3 ligases DCAF15 and CRBN, respectively (Fig. 2), resulting in proteasomal degradation [6]. CRBN-binding compounds (also known as IMiDs) have been shown to recruit and degrade a range of β-hairpin-containing proteins, for example zinc-finger proteins (Fig. 2a) [24]. Indisulam has been shown to degrade a specific protein, an essential mRNA splicing factor RBM39 [25, 26], and form a highly cooperative ternary complex with RBM39 and DCAF15 (Fig. 2b) [27]. In contrast to IMiDs and indisulam, PROTACs can either be cooperative or noncooperative facilitated by the fact they are bifunctional molecules and generally contain two already potent inhibitors linked together in some way. Just as cooperativity facilitates the activity of molecular glues (with often weak binary affinities) and can improve the degradation efficiency of PROTACs [14, 17, 28], the absence of positive cooperativity can still lead to potent degradation [29, 30].

The distinction between PROTACs and molecular glues which recruit E3 ligases is well-understood in chemical terms: PROTACs

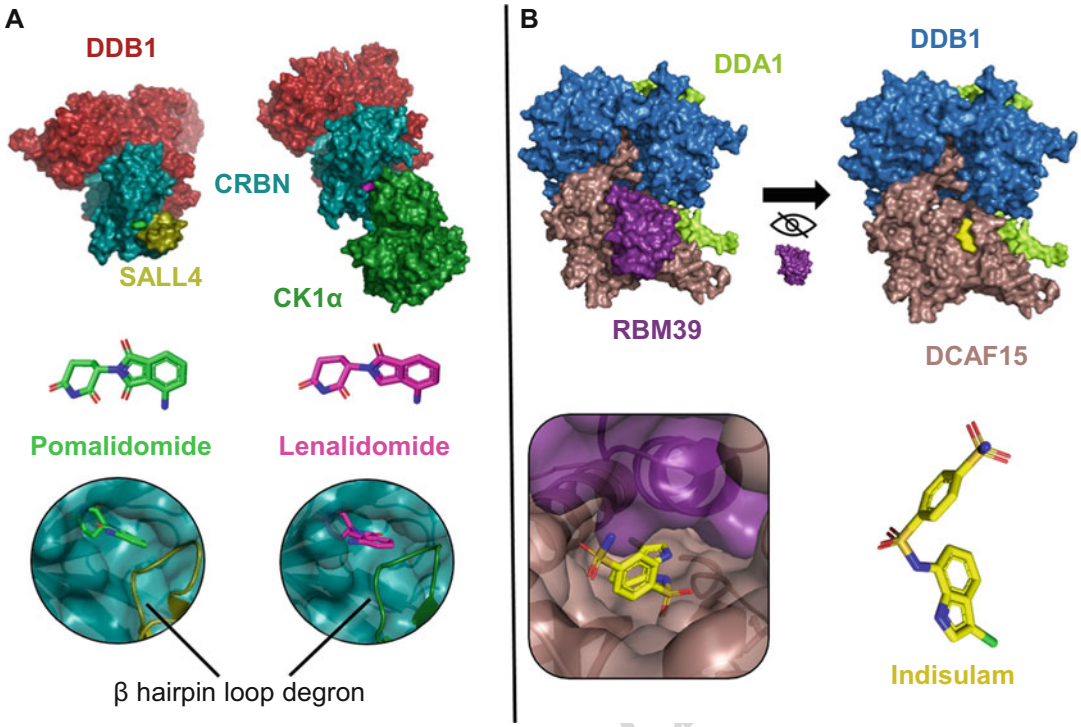

Fig. 2 Comparison of binary and ternary complex formation. (**a**) Depiction of IMiD-based molecular glues Pomalidomide (left) and Lenalidomide (right) which recruit distinct neo-substrates SALL4 and CK1α, respectively, among others. A requirement for neo-substrate recruitment to IMiD is a β hairpin loop which acts as a degron motif. (**b**) Structural basis for RCM39 recruitment to DCAF15 by Indisulam. Top left: full protein complex; top right: RBM39 is hidden to reveal Indisulam which is buried under RBM39 at the interface between it and DCAF15

are bifunctional molecules containing a linker, whereas molecular glues are essentially linker-less PROTACs and lack a target binding moiety. On the other hand, care needs to be taken when developing PROTACs made of E3 ligase binders that are themselves molecular glues, to ascertain the spectrum of potential proteins being degraded. This has been demonstrated by Yang et al. during the development of CRBN-based MDM2 degraders when they identified compound MG-277 which exhibited a high potency in phenotypic cancer cell growth assays despite showing only modest degradation of MDM2 [31]. It was found that the phenotypic activity of the compound was MDM2-independent and was a result of GSPT1 degradation which has also been identified as an off-target of some kinase degraders [32].

1.3 Structural Basis for PROTAC Cooperativity and Selectivity

In much of the early PROTAC literature, the nature of the ternary complex was often depicted as two proteins held spatially apart by a molecule with a linker 'floating' in empty space. This picture changed considerably with the emergence of the first structural

information on PROTAC-induced ternary complexes. In 2017, the structure solution of the BET bromodomain degrader MZ1 in complex with $BRD4^{BD2}$ and VBC (VHL:ElonginB:ElonginC) helped establish a new model for PROTAC-induced ternary complexes [14]. Rather than acting as an inert spacer between the two independent ligands, the linker it was found to coil around itself, aiding formation of a significant protein–protein interaction (PPI) network and a bowl-shaped interface. These de novo PPIs resulted in a stable and cooperative ternary complex ($\alpha = 17.6$) demonstrated by isothermal titration calorimetry (ITC). Perhaps, most interesting was the fact that high cooperativity was not conserved across the BET family proteins, explaining the propensity for MZ1 to preferentially degrade BRD4 over the other bromodomains despite using a pan-BET inhibitor scaffold JQ1 [33]. This was a striking early example of the potential for PROTACs to impact drug discovery. The design of selective BET inhibitors had been challenging the field for years due to the highly conserved acetyllysine binding pocket [34]. By targeting the protein for degradation, the protein surface residues (which are typically much less conserved across protein families) were able to facilitate selectivity by forming de novo PPIs with the E3 ligase. The increased selectivity conferred by PROTAC-mediated degradation has also been demonstrated with the use of VHL and CRBN-recruiting PROTACs based on Foretinib, a nonselective c-MET tyrosine kinase inhibitor [15]. Despite retaining binding to a common set of 51 kinases, the compounds showed vastly different proteome-wide activity, and degradation activity was not found to correlate with binary affinities. In particular, one of the kinase targets (p38alpha) was shown to be effectively degraded in spite of a weak binary binding affinity for the kinase itself.

While these early studies shed light on the thermodynamic and structural properties of PROTAC-induced ternary complexes, it was not until 2019 that the first kinetic studies as evaluated by SPR were published [35]. With the VBC protein complex immobilised on the sensor chip surface Roy et al. studied, the binary and ternary half-lives ($t_{1/2}$) of previously published BET degraders including MZ1. Consistent with the previously discussed thermodynamic data, $BRD4^{BD2}$:MZ1:VBC was shown to form a remarkably stable ternary complex with a $t_{1/2}$ of 130 s compared to the binary (MZ1:VBC) value of 43 s. In addition, cooperativity values were calculated in these experiments which were found to correlate well to previously reported ITC values [14, 28]. This work was further validated later that year when the kinetic findings with MZ1 were independently repeated, along with the characterisation of the potent BET degrader GNE-987 which was shown to form an extremely long-lived complex with VBC and $BRD4^{BD1}$ [36].

Although cooperativity is not a requirement for potent degradation, it can not only facilitate selectivity but also potentially allow

the use of weak ligands. This would potentially allow the degradation of 'undruggable' targets for which only weak ligands exist due to their shallow featureless pockets. If a PROTAC is able to induce productive PPIs and form a cooperative stable ternary complex, these proteins could be targeted; however, it is currently very difficult to predict features which will facilitate this cooperativity. It has been shown in the literature that this is possible. One of the first examples of degradation with a weak E3 ligase ligand was using a PROTAC containing a fluoro-hydroxyproline motif in the VHL binding ligand [37]. Despite the fluorinated VHL binding ligand 14b losing over 20-fold binding affinity with a dissociation constant (K_d) of 3 μM, when conjugated into a 'MZ1-like' PROTAC, it displayed a BRD4 DC_{50} between 10 and 30 nM likely owing to the measured high cooperativity ($\alpha = 14.5$) [37].

In a more recent study, the effect of using weaker VHL ligands in androgen receptor (AR) degraders was evaluated, working back from an already potent degrader [38]. In this case, a set of intentionally weaker VHL ligands were synthesised to obtain ligands with a K_i of 1–3 μM and conjugated to a previously optimised AR warhead-linker combination. Following degradation studies, it was found all the compounds tested could catalyse the degradation of AR protein and further linker optimisation afforded compound ARD-266 which reduces AR protein by >90% at 10 nM.

Both of the examples described imply that weak binary affinity can be compensated for, following PROTAC conjugation, likely due to the formation of a stable and cooperative ternary complex. While this is encouraging for potentially undruggable targets, these cases benefitted from being able to work backwards from an already potent degrader and the knowledge that the system being studied was 'degradable'. In contrast, the prospect of starting with a weak ligand against a difficult target is expected to be challenging but is also one of the most exciting opportunities that a PROTAC approach offers.

1.4 Ternary Complex Structures to Guide PROTAC Design

The ability to generate structural information of PROTAC-induced ternary complexes opens the door for structure-based PROTAC design (SBPD) (Fig. 3). Just as structure-based drug design revolutionised drug discovery, SBPD is expected to aid the currently highly empirical nature of PROTAC design and optimisation. Rather than considering each ligand in isolation, structural information supported by molecular modelling tools allows for optimisation at the PPI interface especially through linker design.

The $BRD4^{BD2}$MZ1:VBC ternary complex structure discussed previously directly facilitated the rational design of novel PROTACs AT1 and MacroPROTAC-1 (Fig. 3a–c) [14, 39]. As the first published example of SBPD, AT1 was designed based on the MZ1 crystal structure which identified the *tert*-leucine group of the VHL warhead as an ideal linkage point that was hypothesised to

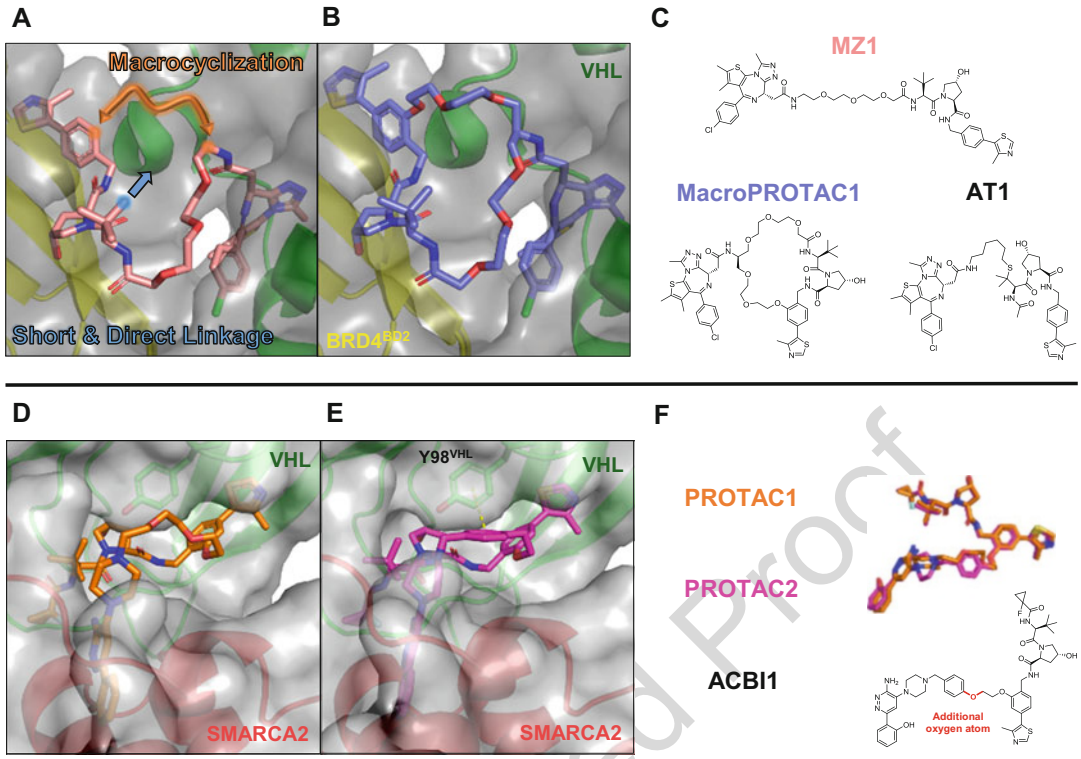

Fig. 3 Structure-based PROTAC design strategies. (**a**) Depiction of design strategies based on the MZ1 ternary crystal structure (PDB: 5T35). (**b**) Ternary crystal structure of MacroPROTAC1 bound to BRD4BD2 and VBC (PDB: 6SIS). (**c**) Chemical structures of the compounds described. (**d**) Ternary crystal structure of PROTAC1 bound to VBC and SMARCA2 (PDB: 6HAY) in which the linker adopts an unfavourable conformation and is pushed against the protein–protein interface. (**e**) Ternary crystal structure of the more potent PROTAC 2 bound to VBC and SMARCA2 (PDB: 6HAX); the more rigid linker now adopts a favourable conformation and forms a T-stacking interaction with Y98VHL. (**f**) Overlay of bioactive conformations PROTAC1 and PROTAC2 is depicted which reveals a good overall conservation of binding mode. Chemical structure of ACBI1, the final optimised PROTAC which differs from PROTAC2 by a single additional oxygen atom in the linker (red) AU3

better discriminate against the crystallographic binding mode and potentially increase selectivity. Following western blotting and unbiased proteomics AT1 was found to exhibit superior selectivity for BRD4 than MZ1 and still retain degradation potency on the face of a fivefold loss of binding affinity at VHL [14]. While the design of MacroPROTAC-1 was based on the same ternary crystal structure, a unique macrocyclisation strategy, supported by in silico calculations, was undertaken in order to lock the PROTAC in the crystallographically observed conformation. Macrocyclisation has been used as a strategy in drug discovery to increase potency and selectivity by reducing the entropic penalty for binding [40]. In the context of a PROTAC with a highly flexible linker, it was hypothesised that locking the PROTAC in its bioactive conformation could be a powerful strategy. In this study, the optimal macrocyclisation

vector and length were predicted computationally, an important step due to the bespoke linker synthesis that was required. Despite a 12-fold loss in binary binding affinity for $BRD4^{BD2}$, MacroPROTAC-1 exhibited comparable degradation activity to MZ1 and the ternary crystal structure confirmed the predicted binding mode (Fig. 3b) [39].

The examples discussed already have been based on the ternary structure of MZ1, a potent and already well-characterised degrader. Structural information has also been leveraged to drive the design of potent PROTACs for SMARCA2 and SMARCA4 proteins [41]. These are subunits of chromatin remodelling BAF/PBAF complexes which have been identified as cancer targets [41]. Although ligands exist for the bromodomains of these proteins, they have been shown to be ineffective as a cancer therapy [42]. In this study, an initial set of PROTACs was synthesised based on a published SMARCA2/4 bromodomain ligand [43] and a potent VHL-recruiting ligand [44]. Despite only partial degradation being observed, biophysical studies were crucial in identifying the most cooperative ligand PROTAC 1 which was co-crystallised with $SMARCA2^{BD}$ and VBC. Inspection of the crystal structure revealed favourable PPIs between $SMARCA2^{BD}$ and VBC; however, it was also observed that the polar polyethylene glycol linker was in a strained conformation and in unfavourable contacts with a hydrophobic interface within the complex (Fig. 3d). Armed with this information, a more lipophilic and rigid linker was designed containing a phenyl ring which could potentially form pi-stacking interactions at the interface. This led to the synthesis of PROTAC 2 and finally ACBI1 following further modification. The ternary crystal structure of PROTAC 2 revealed a similar binding mode of the initial hit and a T-stacking interaction between the linker and Y98 of VHL (Fig. 3e). These compounds displayed significantly improved degradation and were found to be highly cooperative and following proteomics studies ACBI1 was qualified as a potent and selective degrader of SMARCA2, SMARCA4 and PBRM1.

As a result of these important studies, the PROTAC ternary complex is now receiving increased attention within the field. Its characteristics in terms of cooperativity, stability, kinetics and potentially geometry have direct implications for selectivity and potency of target degradation. Currently, PROTAC design is largely empirical in nature, and due to the large number of variables including protein-binding warheads, linkage vectors and the chemical makeup of the linkers themselves, this creates a combinatorially large number of potential PROTACs for synthesis. With all this in mind, being able to measure biophysical parameters and generate structural information is deemed crucial for a guided design, possibly aided by molecular modelling efforts and consequently a much smaller synthesis workload and increased chances of success.

2 Characterisation of Ternary Complexes Using Biophysical Methods

The growing realisation of the important role of the ternary complex in the PROTAC mechanism of action has fuelled the development of new methods or the implementation of existing ones into characterising biophysically PROTAC ternary complexes as a crucial step to evaluate and understand their biological activity. Several biophysical methods have been developed to interrogate PROTAC-induced ternary complex formation both structurally, thermodynamically and kinetically.

2.1 X-Ray Crystallography

X-ray crystallography is a prominent tool in drug discovery to elucidate key structural insights into the binding modes between a small-molecule inhibitor and its target protein. However, crystallographic evidence of the target:PROTAC:E3 ligase long-remained elusive until the first ternary complex crystal structure was solved by Gadd et al. in 2017, as previously described (Fig. 3a) [14].

The methods Gadd et al. used to gain the ternary complex crystal structure of VCB:MZ1:Brd4^{BD2} were to first mix each component, VBC, MZ1 and Brd4^{BD2} in a 1:1:1 stoichiometric ratio to form a ternary complex with final combined concentration of 10 mg/mL. Crystals were then grown using a hanging-drop diffusion format by mixing equal volumes of the ternary complex solution and their crystallisation solution which comprised of 13% (w/v) PEG 8000 precipitating agent and a 0.1 M sodium citrate (pH 6.3) buffer [14]. Similar methods have been used more recently by Testa et al. to elucidate the ternary complex crystal structure of an MZ1 inspired, macrocyclic-PROTAC (Fig. 3b, c) [39], and by Farnaby et al. to crystallise VBC:PROTAC:SMARCA2^{BD} (Fig. 3d–f) [41].

As an additional step in the process, size exclusion gel filtration can be used to purify the ternary complex and separate it from any residual binary complexes and uncomplexed species. However, care should be taken in that the complex is sufficiently stable and not to dissociate significantly during the chromatographic run.

2.2 Proximity Binding Assays

Interrogation of ternary complex formation by proximity-based assays such as amplified luminescent proximity homogeneous assay (AlphaScreen/LISA) and time-resolved fluorescent resonance energy transfer (TR-FRET) provides a high-throughput method of measuring ternary complex formation. Both techniques share a similarity in that they require a donor and an acceptor species. When the donor species is excited by light and brought into close proximity of the acceptor, energy is transferred and light of a particular wavelength is emitted (Fig. 4a). The closer the two counterparts are brought together, the higher and more intense the output signal will be [45–47].

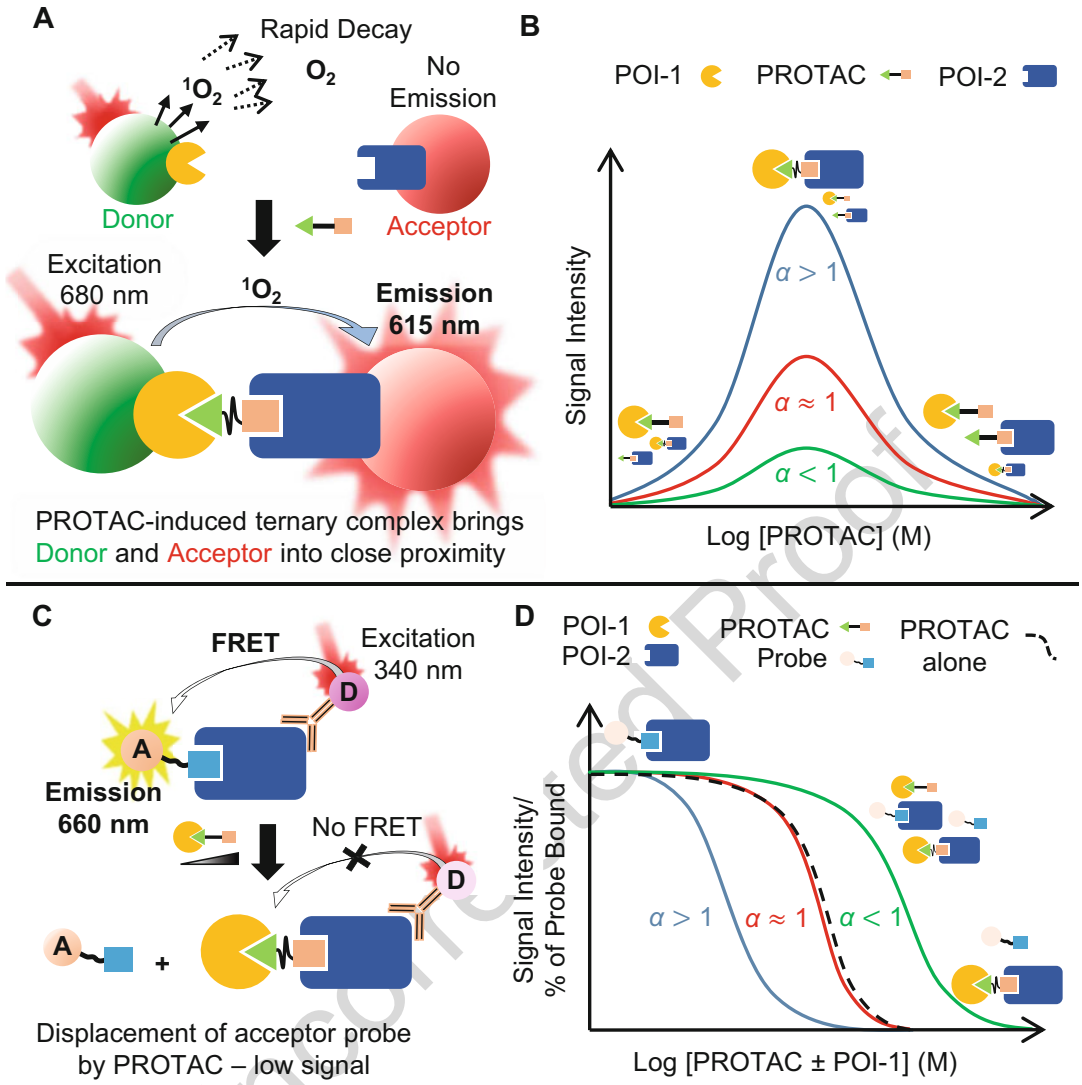

Fig. 4 Schematic representations of proximity-based assays. (**a**) Depiction of an AlphaLISA proximity-based assay. POI-1 and POI-2 are bound to a donor and an acceptor bead, respectively. Fluorescence of wavelength 520–620 nm is emitted as donor and acceptor are brought into close proximity via a PROTAC-induced ternary complex. (**b**) Bell-shaped curve produced from an AlphaLisa assay. As the concentration of PROTAC increases, more ternary complexes form, causing an increase in signal intensity. A decrease of signal is observed due to the characteristic hook effect. Positively cooperative (blue), non-cooperative (red) and negatively cooperative (green) ternary complex proximity profiles are highlighted. (**c**) Depiction of a TR-FRET competition-based assay. When a fluorescently labelled acceptor probe is complexed with POI-2, which in turn is bound to a fluorescent donor probe, a FRET signal is observed as the two fluorophores are in close proximity. No FRET signal is observed when the PROTAC displaces the probe. (**d**) Dose–response curve produced by a TR-FRET competition-based assay. As the concentration of PROTAC alone (black dotted line) or PROTAC:POI-1 complex increases, more fluorescently labelled probe is displaced from POI-2, resulting in a decrease in signal intensity. A rightward shift between binary and ternary binding indicates a negatively cooperative complex (green), no shift indicates a non-cooperative complex (red), and a leftward shift indicates a positively cooperative complex (blue)

The energy transfer process is slightly different between the two assays: AlphaLISA involves the conversion of oxygen into a more excited singlet state caused by laser excitation of a donor bead. This short-lived oxygen species diffuses across to the acceptor bead, activating the fluorophore and causing a fluorescence signal (Fig. 4a) [47]. In the case of TR-FRET, a FRET signal is generated by energy transfer between two complementary fluorophores of different wavelengths after being brought into close proximity (Fig. 4c) [45].

A common use of these proximity-based assays is to assess the relative population and concentration range at which ternary complexes form. To simply monitor PROTAC-induced ternary complex, a PROTAC is usually titrated into a system containing the two protein of interest (POI): POI-1 and POI-2 and their respective reporter species. As the concentration of PROTAC increases, there is a higher population of ternary complexes resulting in a higher output signal until a maxima is reached. It was discovered that more cooperative PROTACs tend to form highly populated ternary species, hence a higher signal intensity spanning over a wider range of concentrations (Fig. 4b) [14].

Gadd et al. developed an AlphaLISA assay to compare the relative ternary complex cooperativities between MZ1, VBC and different BET bromodomains [14]. They demonstrated that more cooperative complexes give a more intense output signal over a wider range of concentrations. To label their proteins, they used Ni-coated acceptor beads and streptavidin-coated donor beads which would bind to His-tagged bromodomains (BD) and biotinylated VBC, respectively. As the PROTAC is titrated into a system containing the individual proteins and respective beads, the ternary complex begins to form. This brings the beads into close proximity and emits fluorescence. As more PROTAC is titrated into the assay, more ternary complexes are formed and a higher intensity signal is received, until the hook effect kicks in. Others have adopted similar approaches to compare other VHL-recruiting degraders, which target other bromodomains such as Brd7/9 [30], and SMARCA2/4 [41], or to analyse CRBN-recruiting BET PROTACs [48, 49].

TR-FRET assays have been widely used to study ternary complexes formed by monovalent molecular glues such as IMiDs with the E3 ligase CRBN and recruited *neo*-substrate proteins [8], and more recently small-molecule enhancers of the oncogenic transcriptional factor, β-Catenin and the $SCF^{\beta\text{-}TrCP}$ E3 ligase [50]. TR-FRET assays have also been used for both CRBN-recruiting [29, 51] and VHL-recruiting degraders [52]. These examples follow a similar set-up whereby one of the target proteins is biotinylated and binds to a terbium or europium-coupled streptavidin donor. The other protein is labelled with an acceptor fluorophore such as BODIPY-FL or Alexa488. The mono- or bivalent

compound is titrated into the system and with increasing concentration, more ternary complexes form which results in a higher signal intensity.

2.3 Competitive and Direct Binding Assays

Although proximity assays offer fast and high-throughput methods for screening ternary complex formation, the bell-shaped curves produced, due to their complexity and overlapping events, are difficult to deconvolute in order to obtain accurate information about binary and ternary affinities and cooperativity. However, these problems can be circumvented by developing competitive and direct binding assays.

Label-dependent binding assays such as fluorescence polarisation (FP), TR-FRET and AlphaLISA among others can be used to gain key binding parameters such as the binary and ternary K_d and so the total ΔG for complex formation between target proteins and PROTACs. Such assays can be separated into two classes: competitive and direct binding assays.

Competition-based assays involve the displacement of a reporter species, usually a labelled small molecule or peptide, from one of the proteins recruited by a PROTAC. In competitive FP assays, as the labelled reporter is displaced by the PROTAC, the signal increases as more reporter species is released into solution. The opposite read-out is true for TR-FRET-based assays as decay in signal is observed due to the reporter no longer being in close proximity/bound for sufficient energy transfer to the fluorophore-containing POI (Fig. 4c). Competitive FP or TR-FRET is commonly used as primary screening assays due to their relative high-throughput prior to more quantitative techniques such as ITC and SPR. Recently, FP assays have been used to determine the stability and cooperativity of ternary complexes formed by different generations of VHL-recruiting PROTACs targeting Brd7/9 [30], and SMARCA2/4 [41]. In these studies, researches compared PROTAC-induced, peptide displacement of a fluorescently labelled HIF-1α (the natural substrate of VHL) bound to VBC in the presence or absence of the target protein. Cooperativity can then be determined by taking the ratio between K_d values—a rightward shift in the displacement profile of binary to ternary binding indicates negative cooperativity, a leftward shift for positive cooperativity, while no change in the displacement profile indicates a noncooperative complex (Fig. 4d). As an orthogonal assay, Farnaby et al. also adopted a competitive TR-FRET-based assay to measure the displacement of a biotinylated SMARCA2 probe in the presence or absence of VBC [41]. A similar competitive displacement approach was adopted for CRBN-recruiting degraders which target Brd4 [51].

AlphaLISA and TR-FRET can provide a direct read-out out in ternary proximity assays and also provide an attractive approach to measure both binary and ternary binding affinities under

competitive modes. Other approaches such as ITC and SPR offer complementary, robust and label-free techniques to directly measure binary and ternary binding affinities and also provide important thermodynamic and kinetic binding parameters [53].

2.4 Isothermal Titration Calorimetry—Thermodynamics

Isothermal titration calorimetry (ITC) assays have been developed to provide a direct, label-free measurement of the thermodynamics of PROTAC-induced ternary complex formation in solution [14]. Key parameters such as associative binding constant (K_a) (and so the dissociation constant, K_d), changes in Gibb's free energy (ΔG) and entropy (ΔS), and also the stoichiometry of binding (N) can all be obtained from a single ITC experiment.

Gadd et al. devised a strategy where they performed reverse titrations POI-1 in the syringe and the PROTAC in the cell, instead of the more common approach involving titrating the small molecule from the syringe into a solution of protein in the cell. This was done to circumvent potential competing equilibria due to the hook effect during the titration. They first titrated POI-1 (BET BDs) into the PROTAC (MZ1) which gave a binary binding affinity for the PROTAC to the target protein ($K_d^{\text{POI-1}}$). This was followed by a further titration of POI-2 (VBC) into the saturated POI-1: PROTAC complex, giving a ternary binding affinity ($K_d^{\text{T, POI-2}}$). Because POI-1 and POI-2 do not interact alone in the absence of the PROTAC, any excess of the unbound POI-1 present in the cell from the first titration will not interfere with the heat signal obtained while titrating POI-2 to form the ternary complex. A separate titration of POI-2 into PROTAC alone is required to get a reference binary binding affinity ($K_d^{\text{POI-2}}$) which can be used to calculate the cooperativity of the ternary complex ($\alpha = K_d^{\text{POI-2}}/K_d^{\text{T,POI-2}}$) [14].

This approach has allowed full thermodynamic characterisation of PROTAC-induced ternary complexes for other VHL-recruiting degraders, which target other bromodomains such as Brd7/9 [30], and SMARCA2/4 [41], as well as PROTACs which dimerise an E3 ligase such as the VHL homo-PROTACs [17]. Although ITC can provide full characterisation of PROTAC-induced ternary complexes, the assay has limited throughput and requires relatively large quantities of material compared to most other assays.

2.4.1 Introduction to Biophysical Characterisation of PROTAC-Induced Ternary Complex Formation by Isothermal Titration Calorimetry Methods

An example of an isothermal titration calorimetry (ITC) procedure to interrogate formation of a ternary complex between VHL-Elongin B-Elongin C complex (VBC), a PROTAC compound, e.g. MZ1 and a BET bromodomain chosen between Brd2-BD1, Brd3-BD1, Brd4-BD1, Brd2-BD2, Brd3-BD2 and Brd4-BD2, is provided, as demonstrated by Gadd et al. in 2017 [14].

2.4.2 Materials

1. ITC Buffer: 20 mM Bis-Tris Propane, pH ~7.4, 150 mM NaCl, 1 mM TCEP.
2. DMSO.
3. POI-1: BET bromodomain (BET BD).
4. POI-2: VBC.
5. PROTAC: MZ1.

2.4.3 Methods

Strategy: the experimental strategy involves running reversed titrations, i.e. POI-1 in the syringe, and PROTAC in the sample cell, to measure binary complex formation. This circumvents issues caused with the hook effect in a ternary titration, whereby the POI-2 is titrated into the remaining solution from the first titration of POI-1 into PROTAC.

Protein Dialysis

1. Prepare 2 L of ITC buffer by first adding 1.5 L of water to a beaker and then bis-tris propane (11.33 g), sodium chloride (17.53 g) and tris(2-carboxyethyl)phosphine hydrochloride (TCEP·HCl) (573 mg). Adjust the pH to 7.4, make the solution up to 2 L in a measuring cylinder with water, transfer to a 2 L beaker, and finally store at 4 °C.
2. Take desired amount of protein (BET BD and VBC) to be used for the following day. Dialyse these proteins in ITC buffer by using low molecular weight (~3.5 kDa) cut-off dialysis tubing, suspended in the 2 L beaker, and stir at 4 °C overnight.
3. Following dialysis, transfer each protein into separate Eppendorf tubes and measure their concentrations in molar by taking three $A_{280\text{nm}}$ measurements per sample, calculating the mean from the three read-outs and then dividing by the protein's extinction coefficient.
4. Take a large amount of dialysis buffer, and transfer to a Falcon tube by filtering through a 0.22 μm syringe filter to use for protein and sample dilutions and for cleaning the sample cell and Hamilton syringes.

PROTAC Preparation

1. Dissolve PROTAC (MZ1) in dimethyl sulfoxide (DMSO) to make a 10 mM stock.
2. For binary titrations between PROTAC and BET BD and for PROTAC and VBC, dilute the 10 mM stock in dialysis buffer by taking 2 μL of the 10 mM stock and adding 998 μL of dialysis buffer to obtain a final PROTAC concentration of 20 μM in ITC buffer and 0.2% (v/v) DMSO.

Protein Preparation

1. Make a 10% (v/v) DMSO stock in dialysis buffer—required for matching up final DMSO concentration at 0.2% (v/v) in samples without PROTACs.

2. Make a 0.2% (v/v) DMSO stock in dialysis buffer—required for control titrations of protein into buffer and buffer into PROTAC and for washing syringe and sample cells between titrations.
3. Make a solution of at least 60 μL of BET BD at a concentration which is tenfold greater than that of the PROTAC (assuming a 1:1 binding stoichiometry), e.g. 200 μM in 0.2% (v/v) DMSO in dialysis buffer. If protein is plentiful, make a 100 μL solution by mixing the correct amount of protein stock with the original dialysis buffer containing NO DMSO to a volume of 98 μL in order to achieve a final concentration of 200 μM. Finally, top up with 2 μL of the 10% (v/v) DMSO in dialysis buffer stock to a total volume of 100 μL.
4. In order to run three VBC titrations with the same protein sample on the same day, make up 200 μL of VBC at 168 μM in 0.2% (v/v) DMSO in dialysis buffer. Do this by adding 4 μL of 10% (v/v) DMSO in dialysis buffer stock and adding the correct amount of protein to dilute to 168 μM. Finally, top up to 200 μL with the original dialysis buffer containing NO DMSO. The final concentration of VBC should be 168 μM due to that being 10× of the concentration at which the PROTAC gets diluted to in the cell at the end of the previous binary titration.

   Note: accurate matching of final DMSO concentration across both sample cell and syringe solutions is critical to ensure high quality of data, as any potential mismatch in DMSO concentration between the two will lead to large heat of dilution from DMSO that can interfere with and even obscure the heat of binding that is to be measured.

Titration Procedure

Titrations are performed using an ITC200 microcalorimeter (GE Healthcare). The titrations are performed in reverse mode (i.e. the protein in the syringe and the ligand in the sample cell). The experiment consists of 19 × 2 μL injections of protein solution at a rate of 0.5 μL/s in 120 s time intervals. An initial 0.4 μL injection of protein is made and discarded during data analysis, as per the manufacturer instruction. The experiments are performed at 25 °C with a stirring speed of 600 rpm.

Notes: Ensure to wash the syringe between titrations, using the dialysis buffer stock with 0.2% (v/v) DMSO.

DO NOT remove the solution remaining in the sample cell after performing a binary titration of protein into PROTAC and prior to performing the ternary titration.

Wash the sample cell after all titration experiments, except when performing a binary titration that needs to be followed by a ternary titration (see above).

Degas all samples briefly under vacuum before loading them into the sample cell or syringe. This procedure will help to minimise the formation of air bubbles during the titration, which can lead to poor data and so ruin the experiment.

Control Titrations

1. Titrate the 0.2% (v/v) DMSO in dialysis buffer stock into 20 μM of PROTAC in 0.2% (v/v) DMSO. Do a separate titration of 0.2% (v/v) DMSO in dialysis buffer stock into 16.8 μM of PROTAC in 0.2% (v/v) DMSO.
2. Titrate 200 μM of BET BD in 0.2% (v/v) DMSO into 0.2% DMSO dialysis buffer stock. Do a separate titration with 168 μM VBC in 0.2% (v/v) DMSO into 0.2% (v/v) DMSO dialysis buffer stock.
3. The data from these control titrations can be used for baseline subtraction in binary and ternary titrations.

Binary BET BD and Ternary Titrations

1. Titrate 200 μM of BET BD into 20 μM of PROTAC. Both were made with 0.2% (v/v) DMSO and dialysis buffer.
2. Wash and dry the syringe and remove the excess solution from the top of the sample cell (as if starting the titration for the first time), and keep to one side in case of issues with the differential power (DP) or air bubbles.
3. Titrate 168 μM of VBC into the sample cell which now contains 16.8 μM of PROTAC + stoichiometric excess of BET BD, remaining from the previous titration, again all in 0.2% (v/v) DMSO and dialysis buffer. This sample cell concentration was calculated as follows.

$$C = (C\_0\ [V]\_cell)/(V\_cell + V\_inj)$$

Co = Initial [PROTAC] in the cell (20 μM).
V_cell = Volume of the sample cell (200.12 μL).
V_inj = Volume of titrant injected initially (38.4 μL).

Note: The experiment is conducted in this way to ensure that >99% of PROTAC is bound to the BET BD prior to injecting VBC into the cell. This experimental set-up assumes that VBC does not interact with the excess BET BD. This assumption can be easily checked by performing a control titration between the two proteins in the absence of PROTAC and comparing the observed heat with that from the corresponding control titration.

VBC Binary Titration

In order to calculate cooperativity (α), a separate binary titration of VBC into PROTAC must be performed.

1. Titrate the 0.2% (v/v) DMSO in dialysis buffer stock into 20 μM of PROTAC in 0.2% (v/v) DMSO.

2. Wash and dry the syringe and remove the excess solution from the top of the sample cell (as if starting the titration for the first time), and keep to one side in case of issues with the DP or air bubbles.
3. Titrate 168 μM of VBC into the diluted PROTAC solution, again all in 0.2% (v/v) DMSO and dialysis buffer.

Data Analysis

Data is usually fitted using a single-binding site model to obtain stoichiometry n, the association constant K_a (from which the dissociation constant K_d can be readily calculated) and the enthalpy of binding ΔH using MicroCal LLC ITC200 Origin software which is provided by the manufacturer. The entropy of binding ΔS is also given by the MicroCal LLC ITC200 Origin software or can be obtained from the binding thermodynamics equation $\Delta S = (\Delta H - \Delta G)/T$, once the free energy ΔG is calculated from the measured K_a using the equation $\Delta G = -RT \times \ln(K_a)$.

2.5 Surface Plasmon Resonance—Kinetics

PROTAC delivers a kinetic cycle of recognition, target ubiquitination and degradation. The kinetics of each individual step in the mechanism therefore are likely to play an important role in the overall efficiency of the process, much as they do in enzyme catalysis [54]. However, until recently, the kinetics of PROTAC-induced ternary complex association and dissociation had not come into focus. This changed with a first study characterising the kinetics of PROTAC ternary complexes using SPR [35].

Similarly to ITC, SPR is a label-free technique which can provide key thermodynamic binding parameters, K_a and K_d, of both binary and ternary complex formation but at a much higher throughput and offering, yet another way of quantifying cooperativity. In addition, SPR offers a unique way of characterising ternary complexes kinetically, by deconvoluting the associative (k_{on}) and dissociative (k_{off}) rate constants of the ternary complex equilibrium (Fig. 5). In 2019, Roy et al. developed the first SPR-based assay to measure the kinetics of PROTAC-induced ternary complexes [35]. They chose to benchmark their assay using the well-characterised PROTAC MZ1, as well as other BET targeting PROTACs which had also been characterised by ITC [14, 28, 35]. They designed a VBC construct which harboured an AviTag sequence on ElonginB for site-specific biotinylation (called 'biotin-VCB'), and expressed, purified and immobilised the resulting biotinylated protein onto a streptavidin-loaded SPR chip. They then measured kinetics of the binary interaction between the immobilised VBC and PROTAC alone or the ternary interaction between the immobilised VBC and the preincubated, PROTAC:BD complex. The experiments revealed that the ternary complexes formed between VBC and MZ1 and $Brd2^{BD2}$ and $Brd4^{BD2}$ had the slowest dissociative half-life (calculated by $t_{1/2} = \ln 2/k_{off}$) of 67 and 130 s,

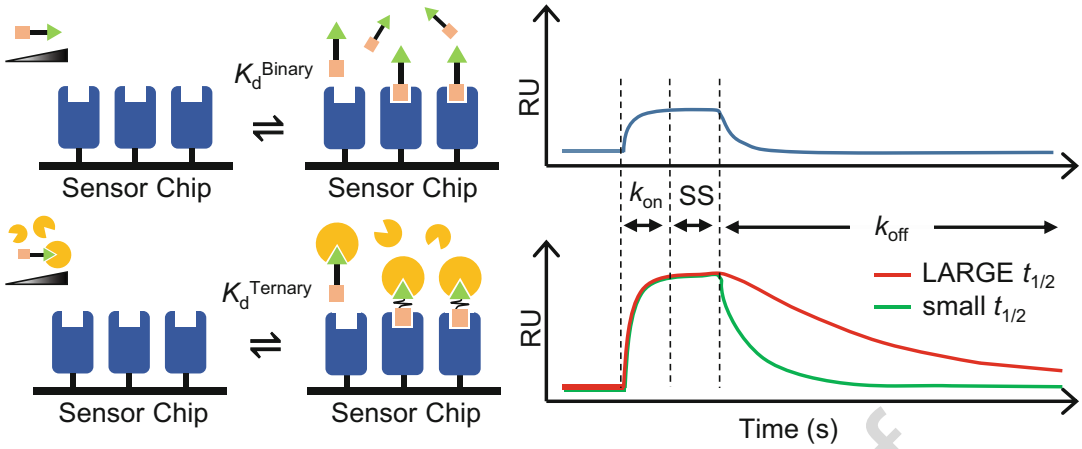

Fig. 5 Schematic representation of an SPR-based assay for binary and ternary complex formation. POI-2 is immobilised onto the sensor chip. For binary experiments (top), varying concentrations of PROTAC are flowed over the POI-2 immobilised surface resulting in a low maximal response (R_{max}) due to the relatively small increase in surface density. For ternary experiments (bottom), varying concentrations of PROTAC:POI-1 complex with excess POI-1 are flowed over the surface resulting in a high Rmax. Examples of binding profiles for a single injection of PROTAC and PROTAC:POI-1 are shown (top right and bottom right, respectively). The ternary binding profile (bottom right) shows a comparison between a ternary complex with a long dissociative half-life ($t_{1/2}$) (red) and a ternary complex with a short $t_{1/2}$ (green). Kinetic parameters: k_{on} (associative rate constant), k_{off} (dissociative rate constant) and SS (steady state) are labelled

respectively, and much slower than $Brd3^{BD2}$ ($t_{1/2}$ = 6 s). Conversely, the fastest dissociating ternary complexes were formed with the first bromodomains (BD1) of Brd2, Brd3 and Brd4 with $t_{1/2}$ < 1 s. Interestingly, the dissociative half-lives of the ternary complexes of VBC:MZ1 with the BD2s were found to correlate with the initial rates of degradation of the different BET proteins, with the most stable and long-lived complexes driving faster rate of target degradation, as a result of a greater level of protein ubiquitination [35]. Overall, these studies are providing emerging evidence that the lifetime and overall stability of the PROTAC ternary complex directly influence the outcome of target protein degradation [41, 35].

More recently, Pillow et al. adopted a similar SPR strategy, where they compare the JQ1-based BET degraders, MZ1 and ARV-771 with their new picomolar potent degrader, GNE-897. The ternary complex between VHL, GNE-897 and $Brd4^{BD1}$ was found to have a dissociative half-life of just over 1 h [36]. These findings again demonstrate the relationship between a long-lived ternary complex and the potency of the degrader molecule.

In vitro biophysical methods offer key mechanistic insights into the way by which we perceive PROTAC-induced ternary complex formation. The techniques described above allow researchers to

fully characterise the formation and dissociation of PROTAC-induced ternary complex both thermodynamically and kinetically. As these techniques use mostly purified, recombinant protein constructs rather than full-length proteins, they provide a first shell of interactions so serve as good a model for how these compounds are behaving within the cell. To understand the full picture of ternary complexes, ultimately similar biophysical techniques and approaches must be incorporated or adapted to work into a more native environment.

3 Cellular and Functional Characterisation of Targeted Protein Degradation Mediated Via Ternary Complex Formation

3.1 Cellular Target Engagement Assays

PROTACs efficacy stems from the productive simultaneous engagement of both target protein and E3 ligase within the ternary complex. Therefore, PROTACs require the procurement of selective ligands for both targets. Conventionally, ligand-target engagement is observed via in vitro biophysical techniques using recombinant proteins; however, these approaches do not replicate the complexity of the intracellular environment adequately. Compound exposure is crucial to cellular target engagement and is affected by permeability, export/efflux, compound sequestration and protein compartmentalisation [55]. Inadequate exposure leads to lower efficacy, typified by compounds with high-affinity in vitro but lower affinity in cellular assays, a phenomenon termed 'cell drop-off' [56].{Swinney, 2004 #4} Cell-based target engagement assays are therefore vital in the development of de novo small-molecule probes and PROTACs in early drug discovery.

3.1.1 Binary Target Engagement

Chemical proteomics approaches have, in recent years, emerged as a powerful method for measuring target engagement in cells. These approaches use occupancy probes that enrich specific target proteins from cell lysate for quantitative mass spectrometry analysis. These probes contain a selectivity handle (against the POI) and a functional moiety for immobilisation or protein isolation, e.g. biotin. The selectivity handle consists of either the compound being assessed (affinity-based probes) or a reactive group that irreversibly binds to the target (activity-based probes). Target engagement is observed through competition against an unmodified compound. Affinity-based probes have previously demonstrated a novel engagement of Bufexamac for HDAC6/HDAC10 [57]. Similarly, fluorophosphate activity-based probe has observed uncharacterised serine hydrolases activity of protein within breast cancer tissue [58]. The improved kinobead solid-supported probes enabled analysis of the interactomes of 243 kinase inhibitors [59].

Advantages of activity−/affinity-based probes include complete proteome analysis within a single experiment and their

applicability in primary and patient-derived cell lines. Proteomic approaches, however, require cell lysis which disrupts the binding equilibria of reversible affinity-based probes. Photo-affinity labelling circumvents this problem via induced UV-mediated photo-crosslinking of a probe to a target protein. Dasatinib and JQ1 inhibitors engagement was investigated using a 2-aryl-5-carboxy-tetrazole (ACT) photo-affinity label approach [60].

The cellular thermal shift assay (CETSA) is an alternative approach that requires no protein or compound modification. CETSA works on the principle of thermodynamic stabilisation induced by compound binding. Molina et al. recognised that compound-mediated thermodynamic stabilisation could be observed in cells and under nonlytic conditions up to 65 °C [61]. The compound-mediated shift in protein aggregation is quantifiable by different methods such as immunoblotting, reporter-based techniques and mass spectrometry. Combining CETSA and chemoproteomics approaches for target engagement, Klaeger et al. assessed the target engagement and selectivity profile of clinical kinase drugs [62]. Limitations of CETSA include the need for affinity reagents, i.e. antibodies, limitations of affinity free approaches, and a bias against protein complexes has been observed. Nanoluciferase thermal shift assay (NaLTSA), which measures thermodynamic stability as a luminescent output, circumvents the need for antibodies and has been implemented to detect inhibitor activity against kinases, bromodomains and HDACs. NaLTSA is amenable for high-throughput experiments making it an appealing alternative to CETSA [63].

Live cell imaging utilising fluorescent occupancy probes are appealing approaches for protein targets intractable to proteomic or thermostability-based methods, e.g. membrane proteins. In this approach, the fluorescent probe acts competitively against a non-derivatised compound added in a dose-dependent manner, as seen with CA200645 fluorescent probe being used to compete against compounds for binding with A3 and A1 receptors [64]. A limitation of fluorescent probes is that they must not be cross-selective as success is dependent on the proximal association of the fluorophore to the correct protein.

A similar approach termed fluorescence anisotropy (FA) or polarisation (FP) can observe compound engagement in live cells. Fluorescent polarisation has been shown at a single-cell resolution for observing ibrutinib and olaparib engagement in cells. The benefit of this approach is the increased spatial resolution, i.e. single-cell microscopy enabled observation of engagement heterogeneity among individual cells [65].

Despite requiring target and compound modification, Foerster resonance energy transfer (FRET) offers a direct, real-time, high-throughput screening approach for observing target engagement in

living cells. A limitation of FRET technologies is that the background fluorescence produces a poor signal-to-noise ratio. Time-resolved FRET (TR-FRET) improves the signal-to-noise ratio by using lanthanides which have an extended fluorescent half-life; however, TR-FRET is considered intractable for intracellular proteins without cell lysis.

An orthogonal approach that is tractable for intracellular proteins in live cells is bioluminescent resonance energy transfer (BRET). BRET uses a bioluminescent protein, such as the luciferase from *Renilla reniformis*, which does not require light excitation and benefits from a low background fluorescence [66]. Unlike TR-FRET, BRET has demonstrated engagement and residence time of HDAC inhibitors; SAHA, FK228 and TDP-A against target HDACs [67].

PROTAC degraders in their own right are emerging as potential chemical tools for target engagement studies. The idea is to derivatise small molecules with suspected target binding affinity into a bifunctional PROTAC molecule in the hope to identify one or more proteins being degraded, e.g. by proteomics, as a read-out for target engagement. This approach was applied to the compound CCT251236 to validate its engagement with the target protein pirin, which was confirmed via converting CCT251236 into a PROTAC and then observing degradation of pirin upon treatment of cells [68].

3.1.2 Target Engagement of the Ternary Complex

The PROTACs ternary complex is the key species in the PROTAC mechanism of action; therefore, understanding the formation efficiency and kinetics of ternary complexes within a cellular context is valuable in guiding structure–activity relationship (SAR) development of PROTAC compounds. Importantly, due to the potential transient and dynamic nature of the ternary complex, direct observation in cells can lead to false negatives results.

Whitworth et al. developed an optimised AlphaLISA assay for observing the ternary complex within cell lysates. PROTAC MZ1-mediated ternary complex formation was probed using ectopically expressed FLAG-tag-conjugated BRD4-BD2 and biotinylated E3 ligase that could complex with a FLAG-tag-coated bead acceptor and streptavidin-coated bead donor. AlphaLISA signal was measured from the close proximity of FLAG-tagged acceptor beads to streptavidin donor beads. This research accomplished the first use of the AlphaLISA assay for observing ternary complex formation using full-length proteins natively expressed within cells [69]. As this is an endpoint assay, this system benefits for a detection mechanism not precluded by the degradation of the target protein; however, real-time observation of the ternary complex cannot be observed using this approach, and it is not generally suited for high-throughput screening applications.

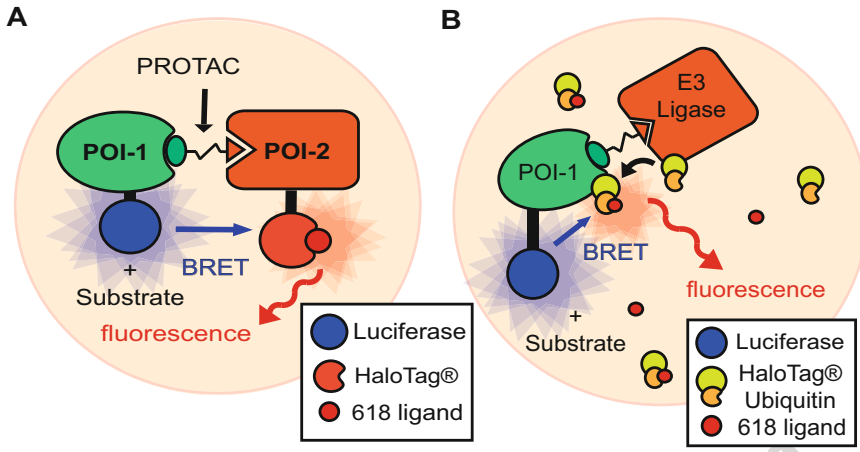

Fig. 6 PROTAC based applications of the NanoBRET experimental platform. (**a**) Application of NanoBRET to determine the extent of PROTAC-mediated ternary complex formation. Fluorescence signal arise when a luminophore-tagged POI and a HaloTag-fused E3 ligase are brought into proximity. (**b**) Application of NanoBRET to determine the extent of PROTAC-induce target ubiquitination. Fluorescence signal arise when a luminophore-tagged POI is covalently modified with an ectopically expressed ubiquitin–HaloTag conjugate. PROTAC compound composed of POI ligand (green circle), E3 ligand (orange triangle) connected by a linker (black), POI (green), E3 (orange), NanoBIT/luciferase (blue), NanoBRET 618 Ligand (red), HaloTag–Ubiquitin (yellow and orange, respectively)

Another approach by Riching et al. uses the previously discussed BRET technology to determine ternary complex formation in living cells [70]. The approach termed NanoBRET utilises a NanoBiT luciferase-tagged protein donor and a HaloTag-conjugated protein labelled with the 618 ligand—a fluorophore-containing chloroalkane handle for use in the HaloTag technology—as the fluorescent acceptor (Fig. 6a). HiBiT, an 11-amino acid peptide tag, was conjugated to the BET proteins BRD2, BRD3 and BRD4. HiBiT complexed with the ectopically expressed LgBIT in a furimazine substrate environment produces luminescence. Cells containing HiBiT-conjugated BET proteins ectopically expressing HaloTag-conjugated VHL or CRBN, LgBIT, furimazine substrate, and 618 Ligand treated with either MZ1 or dBET1 PROTACs were monitored to observe ternary complex formation. The ratiometric nature of this approach makes it suitable for observation of the ternary complex as it is limitedly impacted by protein turnover; however, the addition of a proteasomal inhibitor can increase NanoBRET signal. One limitation of the NanoBRET system is that it has a weaker signal-to-noise ratio compared to non-FRET-based assays.

Phase-shift live cell imaging approaches have been used to observed ternary complex formation of PROTACs targeting BET proteins. SPPIER (separation of phase-based protein interaction reporter) by Chung et al. detected dBET1-, ARV-825 and

ARV-771-mediated ternary complex formation of BRD4 BD1 with their respective E3 ligases [71]. SPPIER functions by the use of EGFP-HOTags conjugated to the interacting partners and upon initiation of a ternary complex induce the formation of a multi-domain complex transforming a defuse EGFP signal into condensed detectable EGFP fluorescent puncta. A limitation of this approach is its low spatial resolution; however, its high brightness, distinct phase change and real-time applicability suggest this approach is amenable to high-throughput screening.

FLOUPPI (fluorescent-based technology detecting protein–protein interaction) approach also utilises phase-shift fluorescent imaging [72]. It involves the co-expression of an Azami-Green (AG)-fused protein and another assembly helper (Ash)-tagged proteins in cells. AG-derived fluorescence is diffuse in the absence of ternary complexing; however, once the engagement is initiated, AG-derived fluorescence produces fluorescent foci through complexing of the two proteins through Ash tags. dBET1 and ARV-825 induced the formation of GFP foci as a result of CRBN: BRD4: PROTAC ternary complex formation. FLOUPPI has a higher spatial resolution compared to SPPIER, enabling FLOUPPI to determine the intracellular localisation of PROTAC-mediated ternary complex formation. A possible limitation of this approach, however, is that nonspecific foci formation can occur as a result of target protein self-oligomerisation, thereby limiting the scope of this approach.

3.2 Cellular Target Ubiquitination and Degradation Assays

Ternary complex formation is a necessary step in the PROTAC mechanism of action, but may not be sufficient for downstream catalysis. Functional PROTACs must be able to induce ubiquitination of their protein targets before degradation can proceed. A PROTACs ability to induce productive ubiquitination is dependent on other factors, such as the relative configuration and stability of the ternary complex produced by a PROTAC, E3 ligase, and the target protein [35, 73]. Therefore, assays that can observe protein ubiquitination & degradation in a cell-based environment are instrumental for developing functional PROTACs.

3.2.1 Assessing Target Ubiquitination in Cells

Conventional methods for determining ubiquitination in PROTAC activity studies involves affinity tag pull-downs, or co-immunoprecipitation of PROTAC-treated cells with a western blot or mass spectrometry-based read-out. The abundance of different types of highly specific ubiquitin antibodies makes this approach amenable to most PROTAC activity studies.

Another aspect of ubiquitination is linkage type, with different linkages and chain lengths/topologies resulting in different cellular responses. Linear K48- and K63-linked ubiquitin strands are commonly studied in PROTAC activity studies since they facilitate recognition by the proteasome, for example, as presented by Chu

et al., demonstrating K48-specific polyubiquitination of Tau using a novel degrader TH006 [74]. Other linkage types are also probed since this can reveal information regarding E3 ligase activity and PROTAC efficacy. As seen when DT2216-mediated degradation of BCL-XL induced Lys 87 ubiquitination [75].

A complementary approach for determining linkage type is to use ectopically overexpressed lysine-substituted ubiquitin mutants. These ubiquitin mutants are deficient in the necessary lysine required for a single linkage type, by probing with different mutants it possible to determine linkage type of an enriched ubiquitinated protein. Ottis et al. demonstrated different ubiquitination linkage types produced by stably expressed E3 ligases–HaloTag conjugates. They concluded that different E3 ligases facilitate different linkage types, as an example, hijacking β-TrCP-induced formation of K48 linkages, while parkin led to K27 and K6 linkages [76].

Riching et al. have also developed two BRET-based assay for determining ubiquitination kinetics using the same HiBiT-BET conjugate donors discussed previously but paired with ectopically overexpressed HaloTag–Ubiquitin conjugate acceptor (Fig. 6b) [70]. In the presence of ligand 618 and ectopically expressed LgBIT, Riching et al. demonstrated rapid and more extensive ubiquitination of BRD2 and BRD4 in the presence of MZ1 PROTAC, relative to BRD3. The orthogonal approach, the NanoBRET™ immunoblot assay, utilises a polyclonal ubiquitin primary antibody and Alexa594-conjugated secondary antibody as an acceptor. Their results showed that both approaches show identical trends to those observed in the HaloTag–Ubiquitin kinetic experiments.

3.2.2 Assessing Protein Degradation in Cells

The last step of the PROTAC mechanism of action is protein degradation, and since functional PROTACs must be able to induce degradation, it is, therefore, imperative to have robust assays in hand to be able to observe degradation dynamics within a cellular context.

Given that the ternary complex has a bell-shaped isotherm, it is important to recognise that false negatives can arise from cellular degradation studies where PROTAC concertation exceeds maximal ternary complex formation, resulting in the 'Hook effect', so dose-dependent experiments are best performed in PROTAC activity studies (Fig. 7).

An important factor in degradation studies is the use of appropriate controls. An important control is the use of inactive PROTAC analogues that, for example, lack binding to the target or E3 ligase, as means to validate PROTAC mechanism of degradation. These are important controls because they control for ternary complex formation, and other artefacts, for example compound

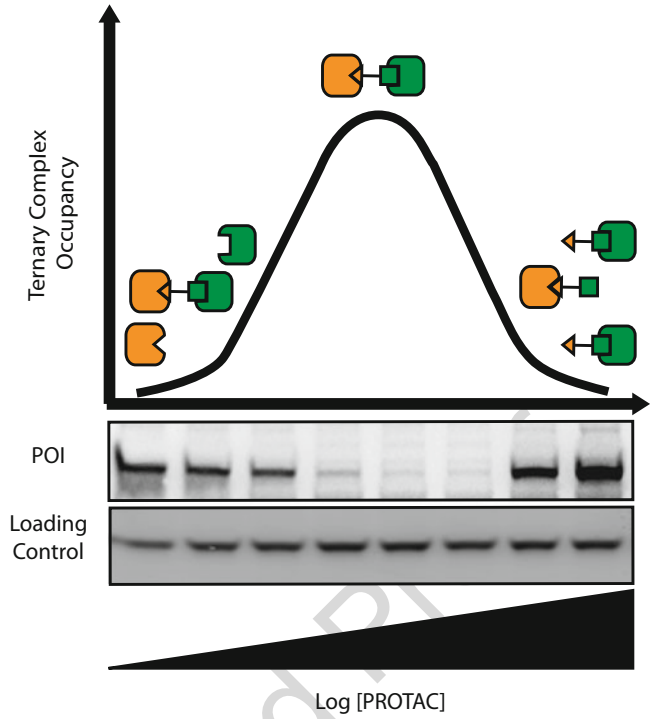

Fig. 7 Hook effect observed in PROTAC-induced protein degradation and ternary complex formation. Representative western blot showing POI protein levels across a serial dilution of PROTAC concentration. The observed degradation effect correlates to the extent of PROTAC-mediated ternary complex formation as represented by the bell-shape curve shown above. PROTAC compound: POI ligand (orange triangle), E3 ligand (green square), connected by a linker; POI (orange), E3 (green)

binding, may destabilise the protein target in a PROTAC independent mechanism. An example of this latter mechanism is the study by Kerres et al., where binding to the BCL6 BTB domain was found to induce BCL6 degradation in a proteasomal-dependent fashion yet via an unknown mechanism [77].

Another parameter that can impact on the observed degradation is the target protein resynthesis rate. Commonly, washout experiments are performed, so that a degraded protein can be observed returning to a native protein level upon removal of the PROTAC compound from the cell medium. To this regards, proteins with a long half-life and so slow resynthesis rate would be expected to recover much slower than proteins with short half-life and fast resynthesis rate. However, even for the same target protein, it can be observed that recovery times can vary with different PROTAC compounds, presumably as the result of different cellular uptake and different ternary complex stabilities for the different

PROTACs [70]. Interestingly, some proteins have an accelerating resynthesis rate as a result of transcriptional upregulation following their cellular depletion. Recent proteomic approaches have enabled precise quantitation of mature proteins separately from nascent proteins, as well as monitoring the proteomic environment upon degrader treatment over time. Savitski et al. using this approach indicated that PROTAC degrader-mediated reduction in BRD2, BRD3 and BRD4 protein levels does not accelerate their resynthesis up to 24 h [78].

Dose dependency, timing, and the extent of degradation induced by PROTACs are the most commonly monitored assessments of PROTAC efficacy in cells. These measurements are typically performed using immunoblotting. Zengerle et al. AU9 demonstrated a standard dose-dependent cell-based immunoblot assay of BET protein expression against treatment with different concentrations of BET PROTAC degraders, which enabled us to identify MZ1, the first BET PROTAC degrader that showed preferential degradation of Brd4 other the other BET proteins Brd2 and Brd3 [33]. This approach is well established within the literature, making it an attractive first approach for determining PROTAC-mediated degradation. There are limitations to using western botting, however, such as its semiquantitate nature, its limited dynamic range for low abundant proteins, the need of specific antibodies and its inability to track degradation in real time or in living cells.

The modern capillary electrophoretic separation technique provided by ProteinSimple can improve upon immunoblotting quantitation and range [79]. Similarly, mass spectrometry can be implemented to improve quantitation in protein degradation studies. However, these techniques are still unable to probe real-time degradation in living cells.

Determining PROTAC degradation in living cells in real time has primarily been performed using ectopically expressed fluorescent protein conjugates. Application of fluorescent conjugates has been demonstrated with MZ1-mediated degradation of GFP-tagged BRD4, and halo-PROTAC-induced degradation of Halo-GFP [33, 80]. While using florescent reporters enables the collection of real-time degradation data, ectopically expressed protein conjugates utilise constitutive promoters, which can mask the real degradation kinetics. Gene tagging of a fluorescent reporter at endogenous level, e.g. using CRISPR-Cas9, can circumvent this issue; however, this requires significant time and effort and also risks altering the endogenous protein expression. An example of this from our own laboratory was described in the recent work by Tovell et al. where our optimised HaloPROTAC-E, a chloroalkane conjugate of high-affinity VHL binder VH298, induced reversible degradation of two HaloTag-tagged proteins, SGK3 and VPS34 [81].

A smaller tag can help reduce the time required in producing tagged protein and is less likely to abrogate protein function. Riching et al. used the NanoLuc split luciferase technology of HiBiT, and LgBIT discussed above to track dBET1- and MZ1-mediated degradation of BET proteins in real time in live cells [70]. The benefit of this approach is the small size of the integrated HiBiT tag, the extended dynamic range, absent the need for specific antibodies, its high resolution, and its real-time application makes it a tractable technology for PROTAC degradation studies.

3.2.3 Assessing Protein Degradation In Vivo

PROTACs are an exciting modality in drug discovery with great potential for therapeutic intervention. Despite this, in-vivo analysis of PROTAC efficacy is still in its infancy. The in-vivo analysis of PROTACs is of increasing importance as the field progresses towards clinical intervention—with two candidates currently in clinical trial: Arvinas's ARV-110 for prostate cancer and ARV-471 for breast cancer. Due to PROTACs typical lack of conformity with Lipinski's rule of five, it is crucial to determine PROTAC bioavailability and therefore in-vivo distribution parameters. The first in-vivo analysis of PROTAC efficacy was performed in 2015 in mice by two independent groups, where one explored the protein expression of εRRα after treatment of 100 mg/kg εRRα PROTAC in mouse heart and kidney cell and the other group determined tumour volume reduction in explanted MV4:11 cell in a mouse hind limb in response to DBET1 targeting of BET proteins [13, 82]. These initial in-vivo experiments established PROTAC efficacy via its impact on explanted tumour growth and determining endogenous mouse proteins levels using immunoblotting or proteomics approaches, however, were still limited to intraperitoneal or intravenous routes of administration. More recently, Sun et al. demonstrated both intraperitoneal and oral administration of FKBP12 degrader mediated rapid, and reversible FKBP12 degradation in mice and highlighted the clinical potential of oral administration of PROTACs [83]. This is now established as several orally bioavailable PROTACs have entered the clinic [84].

One recent development has been the utilisation of luciferase tagging to determine PROTAC efficacy in vivo using noninvasive bioluminescent imaging. Bioluminescent imaging is a powerful noninvasive optical imaging technique that works well in whole-murine models due to their naturally low intrinsic bioluminescence and that luminescence is penetrant up to several centimetres. An example of this approach enabled observation of real-time degradation of an FKBP12-conjugated luciferase in MV4;11 cells explanted into mice by novel VHL degrader compounds [85].

4 Concluding Remarks

The catalytic, substoichiometric mode of action of PROTAC is underpinned by the ternary complexes they form with the target protein that is intended to be ubiquitinated and degraded and the recruited E3 ubiquitin ligase. Consequently, the ternary complex is a key intermediate species required for PROTAC mode of action. Despite this, the prevailing approach in the field has been to measuring directly and almost exclusively the final outcome, i.e. protein degradation, often coupled with measurement of binary inhibition/binding at the respective target and E3 ligase. However, recent studies have highlighted that ternary complex stability, cooperativity, kinetics and potentially geometry are emerging and important features that drive potency and efficiency of PROTAC-induced target degradation. As a result, much attention is now being devoted to approaches to studying the thermodynamics, kinetics and structural features of ternary complex formation equilibria and how these influence cellular activities. Here, we cover the key principles and methods being used to understand and study PROTAC ternary complexes and some of the key studies that have led to their current development. We advocate that these approaches and methods should instead be much more mainstream and be part of screening cascades to help guide and drive PROTAC design and characterisation campaigns. We anticipate that studies of ternary complexes and PROTAC mode of action will provide a fertile and exciting area of focus for important advances and method development in future.

Acknowledgements and Funding

We would like to thank many members of the Ciulli group for helpful discussions. We apologise to the authors of many studies in the field which could not be mentioned due to space restriction. The Ciulli laboratory's work on PROTACs has received funding from the European Research Council (ERC) under the European Union's Seventh Framework Programme (FP7/2007-2013) as a Starting Grant to A.C. (grant agreement No. ERC-2012-StG-311460 DrugE3CRLs). R.C. is funded by a PhD studentship from the UK Biotechnology and Biological Sciences Research Council (BBSRC) under the EastBio doctoral training programme (BB/M010996/1). A.B. is funded by a PhD studentship from the Medical Research Scotland (MRS) (1170-2017). C.C. is funded by a PhD studentship from the UK Medical Research Council (MRC) under the doctoral training programme in Quantitative and Interdisciplinary approaches to biomedical science (QI Biomed) (MR/N0123735/1). The Ciulli laboratory receives or has received

sponsored research support from Boehringer Ingelheim, Eisai, Nurix, Ono Pharmaceuticals and Amphista Therapeutics.

Conflict of interest statement: A.C. is the scientific founder, shareholder, nonexecutive director and consultant of Amphista Therapeutics, a company that is developing targeted protein degradation therapeutic platforms. The remaining author reports no competing interests.

References

1. Hill AV (1910) The possible effects of the aggregation of the molecules of haemoglobin on its dissociation curves. J Physiol Lond 40:4–7
2. Labrijn AF, Janmaat ML, Reichert JM, Parren P (2019) Bispecific antibodies: a mechanistic review of the pipeline. Nat Rev Drug Discov 18(8):585–608. https://doi.org/10.1038/s41573-019-0028-1
3. Profit AA, Lee TR, Lawrence DS (1999) Bivalent inhibitors of protein tyrosine kinases. J Am Chem Soc 121(2):280–283. https://doi.org/10.1021/ja983515n
4. Tanaka M, Roberts JM, Seo HS, Souza A, Paulk J, Scott TG, DeAngelo SL, Dhe-Paganon S, Bradner JE (2016) Design and characterization of bivalent BET inhibitors. Nat Chem Biol 12(12):1089–1096. https://doi.org/10.1038/Nchembio.2209
5. Waring MJ, Chen HW, Rabow AA, Walker G, Bobby R, Boiko S, Bradbury RH, Callis R, Clark E, Dale I, Daniels DL, Dulak A, Flavell L, Holdgate G, Jowitt TA, Kikhney A, McAlister M, Mendez J, Ogg D, Patel J, Petteruti P, Robb GR, Robers MB, Saif S, Stratton N, Svergun DI, Wang WX, Whittaker D, Wilson DM, Yao Y (2016) Potent and selective bivalent inhibitors of BET bromodomains. Nat Chem Biol 12(12):1097–1104. https://doi.org/10.1038/Nchembio.2210
6. Che Y, Gilbert AM, Shanmugasundaram V, Noe MC (2018) Inducing protein-protein interactions with molecular glues. Bioorg Med Chem Lett 28(15):2585–2592. https://doi.org/10.1016/j.bmcl.2018.04.046
7. Sun X, Gao H, Yang Y, He M, Wu Y, Song Y, Tong Y, Rao Y (2019) PROTACs: great opportunities for academia and industry. Signal Transduct Target Ther 4:64. https://doi.org/10.1038/s41392-019-0101-6
8. Petzold G, Fischer ES, Thomä NH (2016) Structural basis of lenalidomide-induced CK1α degradation by the CRL4CRBN ubiquitin ligase. Nature 532(7597):127–130. https://doi.org/10.1038/nature16979
9. Douglass EF Jr, Miller CJ, Sparer G, Shapiro H, Spiegel DA (2013) A comprehensive mathematical model for three-body binding equilibria. J Am Chem Soc 135(16):6092–6099. https://doi.org/10.1021/ja311795d
10. Mack ET, Perez-Castillejos R, Suo Z, Whitesides GM (2008) Exact analysis of ligand-induced dimerization of monomeric receptors. Anal Chem 80(14):5550–5555. https://doi.org/10.1021/ac800578w
11. Buxton BH (1905) Bacteriolytic power of immune serum and the theory of complement diversion. J Med Res 13(5):431–459
12. Mulgrew K, Kinneer K, Yao XT, Ward BK, Damschroder MM, Walsh B, Mao SY, Gao C, Kiener PA, Coats S, Kinch MS, Tice DA (2006) Direct targeting of alphavbeta3 integrin on tumor cells with a monoclonal antibody, Abegrin. Mol Cancer Ther 5(12):3122–3129. https://doi.org/10.1158/1535-7163.MCT-06-0356
13. Bondeson DP, Mares A, Smith IE, Ko E, Campos S, Miah AH, Mulholland KE, Routly N, Buckley DL, Gustafson JL, Zinn N, Grandi P, Shimamura S, Bergamini G, Faelth-Savitski M, Bantscheff M, Cox C, Gordon DA, Willard RR, Flanagan JJ, Casillas LN, Votta BJ, den Besten W, Famm K, Kruidenier L, Carter PS, Harling JD, Churcher I, Crews CM (2015) Catalytic in vivo protein knockdown by small-molecule PROTACs. Nat Chem Biol 11(8):611–617. https://doi.org/10.1038/nchembio.1858
14. Gadd MS, Testa A, Lucas X, Chan KH, Chen W, Lamont DJ, Zengerle M, Ciulli A (2017) Structural basis of PROTAC cooperative recognition for selective protein degradation. Nat Chem Biol 13(5):514–521. https://doi.org/10.1038/nchembio.2329
15. Bondeson DP, Smith BE, Burslem GM, Buhimschi AD, Hines J, Jaime-Figueroa S,

Wang J, Hamman BD, Ishchenko A, Crews CM (2018) Lessons in PROTAC design from selective degradation with a promiscuous warhead. Cell Chem Biol 25(1):78–87. e75. https://doi.org/10.1016/j.chembiol.2017.09.010

16. Roy RD, Rosenmund C, Stefan MI (2017) Cooperative binding mitigates the high-dose hook effect. BMC Syst Biol 11(1):74. https://doi.org/10.1186/s12918-017-0447-8
17. Maniaci C, Hughes SJ, Testa A, Chen WZ, Lamont DJ, Rocha S, Alessi DR, Romeo R, Ciulli A (2017) Homo-PROTACs: bivalent small-molecule dimerizers of the VHL E3 ubiquitin ligase to induce self-degradation. Nat Commun 8(1):830. https://doi.org/10.1038/s41467-017-00954-1
18. Steinebach C, Lindner S, Udeshi ND, Mani DC, Kehm H, Kopff S, Carr SA, Gutschow M, Kronke J (2018) Homo-PROTACs for the chemical knockdown of Cereblon. ACS Chem Biol 13(9):2771–2782. https://doi.org/10.1021/acschembio.8b00693
19. Saline M, Rodstrom KEJ, Fischer G, Orekhov VY, Karlsson BG, Lindkvist-Petersson K (2010) The structure of superantigen complexed with TCR and MHC reveals novel insights into superantigenic T cell activation. Nat Commun 1:119. https://doi.org/10.1038/ncomms1117
20. Andersen PS, Schuck P, Sundberg EJ, Geisler C, Karjalainen K, Mariuzza RA (2002) Quantifying the energetics of cooperativity in a ternary protein complex. Biochemistry 41(16):5177–5184. https://doi.org/10.1021/bi0200209
21. Choi JW, Chen J, Schreiber SL, Clardy J (1996) Structure of the FKBP12-rapamycin complex interacting with the binding domain of human FRAP. Science 273(5272):239–242. https://doi.org/10.1126/science.273.5272.239
22. Kepinski S, Leyser O (2005) The Arabidopsis F-box protein TIR1 is an auxin receptor. Nature 435(7041):446–451. https://doi.org/10.1038/nature03542
23. Banaszynski LA, Liu CW, Wandless TJ (2005) Characterization of the FKBP center dot rapamycin center dot FRB ternary complex. J Am Chem Soc 127(13):4715–4721. https://doi.org/10.1021/ja043277y
24. Chamberlain PP, Cathers BE (2019) Cereblon modulators: low molecular weight inducers of protein degradation. Drug Discov Today Technol 31:29–34. https://doi.org/10.1016/j.ddtec.2019.02.004
25. Han T, Goralski M, Gaskill N, Capota E, Kim J, Ting TC, Xie Y, Williams NS, Nijhawan D (2017) Anticancer sulfonamides target splicing by inducing RBM39 degradation via recruitment to DCAF15. Science 356(6336):eaal3755. https://doi.org/10.1126/science.aal3755
26. Uehara T, Minoshima Y, Sagane K, Sugi NH, Mitsuhashi KO, Yamamoto N, Kamiyama H, Takahashi K, Kotake Y, Uesugi M, Yokoi A, Inoue A, Yoshida T, Mabuchi M, Tanaka A, Owa T (2017) Selective degradation of splicing factor CAPERalpha by anticancer sulfonamides. Nat Chem Biol 13(6):675–680. https://doi.org/10.1038/nchembio.2363
27. Bussiere DE, Xie LL, Srinivas H, Shu W, Burke A, Be C, Zhao JP, Godbole A, King D, Karki RG, Hornak V, Xu FM, Cobb J, Carte N, Frank AO, Frommlet A, Graff P, Knapp M, Fazal A, Okram B, Jiang SC, Michellys PY, Beckwith R, Voshol H, Wiesmann C, Solomon JM, Paulk J (2020) Structural basis of indisulam-mediated RBM39 recruitment to DCAF15 E3 ligase complex. Nat Chem Biol 16(1):15–23. https://doi.org/10.1038/s41589-019-0411-6
28. Chan KH, Zengerle M, Testa A, Ciulli A (2018) Impact of target warhead and linkage vector on inducing protein degradation: comparison of Bromodomain and extra-terminal (BET) degraders derived from Triazolodiazepine (JQ1) and Tetrahydroquinoline (I-BET726) BET inhibitor scaffolds. J Med Chem 61(2):504–513. https://doi.org/10.1021/acs.jmedchem.6b01912
29. Zorba A, Nguyen C, Xu Y, Starr J, Borzilleri K, Smith J, Zhu H, Farley KA, Ding W, Schiemer J, Feng X, Chang JS, Uccello DP, Young JA, Garcia-Irrizary CN, Czabaniuk L, Schuff B, Oliver R, Montgomery J, Hayward MM, Coe J, Chen J, Niosi M, Luthra S, Shah JC, El-Kattan A, Qiu X, West GM, Noe MC, Shanmugasundaram V, Gilbert AM, Brown MF, Calabrese MF (2018) Delineating the role of cooperativity in the design of potent PROTACs for BTK. Proc Natl Acad Sci U S A 115(31):E7285–E7292. https://doi.org/10.1073/pnas.1803662115
30. Zoppi V, Hughes SJ, Maniaci C, Testa A, Gmaschitz T, Wieshofer C, Koegl M, Riching KM, Daniels DL, Spallarossa A, Ciulli A (2019) Iterative design and optimization of initially inactive proteolysis targeting chimeras (PROTACs) identify VZ185 as a potent, fast, and selective von Hippel-Lindau (VHL) based dual degrader probe of BRD9 and BRD7. J Med Chem 62(2):699–726. https://doi.org/10.1021/acs.jmedchem.8b01413

31. Yang JL, Li YB, Aguilar A, Liu ZM, Yang CY, Wang SM (2019) Simple structural modifications converting a Bona fide MDM2 PROTAC degrader into a molecular glue molecule: a cautionary tale in the design of PROTAC degraders. J Med Chem 62(21):9471–9487. https://doi.org/10.1021/acs.jmedchem.9b00846
32. Ishoey M, Chorn S, Singh N, Jaeger MG, Brand M, Paulk J, Bauer S, Erb MA, Parapatics K, Muller AC, Bennett KL, Ecker GF, Bradner JE, Winter GE (2018) Translation termination factor GSPT1 is a phenotypically relevant off-target of heterobifunctional Phthalimide degraders. ACS Chem Biol 13 (3):553–560. https://doi.org/10.1021/acschembio.7b00969
33. Zengerle M, Chan KH, Ciulli A (2015) Selective small molecule induced degradation of the BET Bromodomain protein BRD4. ACS Chem Biol 10(8):1770–1777. https://doi.org/10.1021/acschembio.5b00216
34. Baud MGJ, Lin-Shiao E, Cardote T, Tallant C, Pschibul A, Chan KH, Zengerle M, Garcia JR, Kwan TT, Ferguson FM, Ciulli A (2014) Chemical biology. A bump-and-hole approach to engineer controlled selectivity of BET bromodomain chemical probes. Science 346 (6209):638–641. https://doi.org/10.1126/science.1249830
35. Roy MJ, Winkler S, Hughes SJ, Whitworth C, Galant M, Farnaby W, Rumpel K, Ciulli A (2019) SPR-measured dissociation kinetics of PROTAC ternary complexes influence target degradation rate. ACS Chem Biol 14 (3):361–368. https://doi.org/10.1021/acschembio.9b00092
36. Pillow TH, Adhikari P, Blake RA, Chen J, Del Rosario G, Deshmukh G, Figueroa I, Gascoigne KE, Kamath AV, Kaufman S, Kleinheinz T, Kozak KR, Latifi B, Leipold DD, Sing Li C, Li R, Mulvihill MM, O'Donohue A, Rowntree RK, Sadowsky JD, Wai J, Wang X, Wu C, Xu Z, Yao H, Yu SF, Zhang D, Zang R, Zhang H, Zhou H, Zhu X, Dragovich PS (2020) Antibody conjugation of a chimeric BET degrader enables in vivo activity. ChemMedChem 15(1):17–25. https://doi.org/10.1002/cmdc.201900497
37. Testa A, Lucas X, Castro GV, Chan KH, Wright JE, Runcie AC, Gadd MS, Harrison WTA, Ko EJ, Fletcher D, Ciulli A (2018) 3-Fluoro-4-hydroxyprolines: synthesis, conformational analysis, and Stereoselective recognition by the VHL E3 ubiquitin ligase for targeted protein degradation. J Am Chem Soc 140 (29):9299–9313. https://doi.org/10.1021/jacs.8b05807
38. Han X, Zhao L, Xiang W, Qin C, Miao B, Xu T, Wang M, Yang CY, Chinnaswamy K, Stuckey J, Wang S (2019) Discovery of highly potent and efficient PROTAC degraders of androgen receptor (AR) by employing weak binding affinity VHL E3 ligase ligands. J Med Chem 62(24):11218–11231. https://doi.org/10.1021/acs.jmedchem.9b01393
39. Testa A, Hughes SJ, Lucas X, Wright JE, Ciulli A (2020) Structure-based Design of a Macrocyclic PROTAC. Angew Chem Int Edit 59 (4):1727–1734. https://doi.org/10.1002/anie.201914396
40. Soumana DI, Yilmaz NK, Prachanronarong KL, Aydin C, Ali A, Schiffer CA (2016) Structural and thermodynamic effects of macrocyclization in HCV NS3/4A inhibitor MK-5172. ACS Chem Biol 11(4):900–909. https://doi.org/10.1021/acschembio.5b00647
41. Farnaby W, Koegl M, Roy MJ, Whitworth C, Diers E, Trainor N, Zollman D, Steurer S, Karolyi-Oezguer J, Riedmueller C, Gmaschitz T, Wachter J, Dank C, Galant M, Sharps B, Rumpel K, Traxler E, Gerstberger T, Schnitzer R, Petermann O, Greb P, Weinstabl H, Bader G, Zoephel A, Weiss-Puxbaum A, Ehrenhofer-Wolfer K, Wohrle S, Boehmelt G, Rinnenthal J, Arnhof H, Wiechens N, Wu MY, Owen-Hughes T, Ettmayer P, Pearson M, McConnell DB, Ciulli A (2019) BAF complex vulnerabilities in cancer demonstrated via structure-based PROTAC design. Nat Chem Biol 15(7):672–680. https://doi.org/10.1038/s41589-019-0294-6
42. Vangamudi B, Paul TA, Shah PK, Kost-Alimova M, Nottebaum L, Shi X, Zhan YA, Leo E, Mahadeshwar HS, Protopopov A, Futreal A, Tieu TN, Peoples M, Heffernan TP, Marszalek JR, Toniatti C, Petrocchi A, Verhelle D, Owen DR, Draetta G, Jones P, Palmer WS, Sharma S, Andersen JN (2015) The SMARCA2/4 ATPase domain surpasses the Bromodomain as a drug target in SWI/SNFMutant cancers: insights from cDNA rescue and PFI-3 inhibitor studies. Cancer Res 75(18):3865–3878. https://doi.org/10.1158/0008-5472.Can-14-3798
43. Albrecht B, Cote A, Crawford T, Duplessis M, Good A, Leblanc Y, Magnuson S, Nasveschuk C, Romero F, Tang Y (2016) Therapeutic pyridazine compounds and uses thereof WIPO patent WO2016138114
44. Soares P, Gadd MS, Frost J, Galdeano C, Ellis L, Epemolu O, Rocha S, Read KD, Ciulli A (2018) Group-based optimization of potent and cell-active inhibitors of the von Hippel-Lindau (VHL) E3 ubiquitin ligase: structure-

activity relationships leading to the chemical probe (2S,4R)-1-((S)-2-(1-Cyanocyclopropanecarboxamido)-3,3-dimethylbutanoyl)-4-hydroxy-N-(4-(4-methylthiazol-5-yl)benzyl)pyrrolidine-2-carboxamide (VH298). J Med Chem 61(2):599–618. https://doi.org/10.1021/acs.jmedchem.7b00675

45. Lebakken CS, Riddle SM, Singh U, Frazee WJ, Eliason HC, Gao Y, Reichling LJ, Marks BD, Vogel KW (2009) Development and applications of a broad-coverage, TR-FRET-based kinase binding assay platform. J Biomol Screen 14(8):924–935. https://doi.org/10.1177/1087057109339207
46. Glickman JF, Wu X, Mercuri R, Illy C, Bowen BR, He Y, Sills M (2002) A comparison of ALPHAScreen, TR-FRET, and TRF as assay methods for FXR nuclear receptors. J Biomol Screen 7(1):3–10. https://doi.org/10.1177/108705710200700102
47. Beaudet L, Rodriguez-Suarez R, Venne M-H, Caron M, Bédard J, Brechler V, Parent S, Bielefeld-Sévigny M (2008) AlphaLISA immunoassays: the no-wash alternative to ELISAs for research and drug discovery. Nat Methods 5(12):A10
48. Winter GE, Mayer A, Buckley DL, Erb MA, Roderick JE, Vittori S, Reyes JM, di Iulio J, Souza A, Ott CJ, Roberts JM, Zeid R, Scott TG, Paulk J, Lachance K, Olson CM, Dastjerdi S, Bauer S, Lin CY, Gray NS, Kelliher MA, Churchman LS, Bradner JE (2017) BET Bromodomain proteins function as master transcription elongation factors independent of CDK9 recruitment. Mol Cell 67(1):5–18. e19. https://doi.org/10.1016/j.molcel.2017.06.004
49. Wurz RP, Dellamaggiore K, Dou H, Javier N, Lo M-C, McCarter JD, Mohl D, Sastri C, Lipford JR, Cee VJ (2018) A "click chemistry platform" for the rapid synthesis of bispecific molecules for inducing protein degradation. J Med Chem 61(2):453–461. https://doi.org/10.1021/acs.jmedchem.6b01781
50. Simonetta KR, Taygerly J, Boyle K, Basham SE, Padovani C, Lou Y, Cummins TJ, Yung SL, von Soly SK, Kayser F, Kuriyan J, Rape M, Cardozo M, Gallop MA, Bence NF, Barsanti PA, Saha A (2019) Prospective discovery of small molecule enhancers of an E3 ligase-substrate interaction. Nat Commun 10(1):1402. https://doi.org/10.1038/s41467-019-09358-9
51. Nowak RP, DeAngelo SL, Buckley D, He Z, Donovan KA, An J, Safaee N, Jedrychowski MP, Ponthier CM, Ishoey M, Zhang T, Mancias JD, Gray NS, Bradner JE, Fischer ES (2018) Plasticity in binding confers selectivity in ligand-induced protein degradation. Nat Chem Biol 14(7):706–714. https://doi.org/10.1038/s41589-018-0055-y
52. Hsu JH-R, Rasmusson T, Robinson J, Pachl F, Read J, Kawatkar S, O'Donovan DH, Bagal S, Code E, Rawlins P, Argyrou A, Tomlinson R, Gao N, Zhu X, Chiarparin E, Jacques K, Shen M, Woods H, Bednarski E, Wilson DM, Drew L, Castaldi MP, Fawell S, Bloecher A (2020) EED-targeted PROTACs degrade EED, EZH2, and SUZ12 in the PRC2 complex. Cell Chem Biol 27(1):41–46.e17. https://doi.org/10.1016/j.chembiol.2019.11.004
53. Ciulli A (2013) Biophysical screening for the discovery of small-molecule ligands. In: Williams MA, Daviter T (eds) Protein-ligand interactions: methods and applications. Humana Press, Totowa, NJ, pp 357–388. https://doi.org/10.1007/978-1-62703-398-5_13
54. Fisher SL, Phillips AJ (2018) Targeted protein degradation and the enzymology of degraders. Curr Opin Chem Biol 44:47–55. https://doi.org/10.1016/j.cbpa.2018.05.004
55. Hann MM, Simpson GL (2014) Intracellular drug concentration and disposition–the missing link? Methods 68(2):283–285. https://doi.org/10.1016/j.ymeth.2014.05.009
56. Swinney DC (2004) Biochemical mechanisms of drug action: what does it take for success? Nat Rev Drug Discov 3(9):801–808. https://doi.org/10.1038/nrd1500
57. Bantscheff M, Hopf C, Savitski MM, Dittmann A, Grandi P, Michon A-M, Schlegl J, Abraham Y, Becher I, Bergamini G, Boesche M, Delling M, Dümpelfeld B, Eberhard D, Huthmacher C, Mathieson T, Poeckel D, Reader V, Strunk K, Sweetman G, Kruse U, Neubauer G, Ramsden NG, Drewes G (2011) Chemoproteomics profiling of HDAC inhibitors reveals selective targeting of HDAC complexes. Nat Biotechnol 29(3):255–265. https://doi.org/10.1038/nbt.1759
58. Jessani N, Niessen S, Wei BQ, Nicolau M, Humphrey M, Ji Y, Han W, Noh D-Y, Yates JR, Jeffrey SS, Cravatt BF (2005) A streamlined platform for high-content functional proteomics of primary human specimens. Nat Methods 2(9):691–697. https://doi.org/10.1038/nmeth778
59. Médard G, Pachl F, Ruprecht B, Klaeger S, Heinzlmeir S, Helm D, Qiao H, Ku X, Wilhelm M, Kuehne T, Wu Z, Dittmann A, Hopf C, Kramer K, Kuster B (2015) Optimized chemical proteomics assay for kinase inhibitor profiling. J Proteome Res 14

(3):1574–1586. https://doi.org/10.1021/pr5012608

60. AS H, Marjanovic J, Lewandowski TM, Marin V, Patterson M, Miesbauer L, Ready D, Williams J, Vasudevan A, Lin Q (2016) 2-Aryl-5-carboxytetrazole as a new photoaffinity label for drug target identification. J Am Chem Soc 138(44):14609–14615. https://doi.org/10.1021/jacs.6b06645
61. Molina DM, Jafari R, Ignatushchenko M, Seki T, Larsson EA, Dan C, Sreekumar L, Cao Y, Nordlund P (2013) Monitoring drug target engagement in cells and tissues using the cellular thermal shift assay. Science 341 (6141):84–87
62. Klaeger S, Heinzlmeir S, Wilhelm M, Polzer H, Vick B, Koenig PA, Reinecke M, Ruprecht B, Petzoldt S, Meng C, Zecha J, Reiter K, Qiao H, Helm D, Koch H, Schoof M, Canevari G, Casale E, Depaolini SR, Feuchtinger A, Wu Z, Schmidt T, Rueckert L, Becker W, Huenges J, Garz AK, Gohlke BO, Zolg DP, Kayser G, Vooder T, Preissner R, Hahne H, Tõnisson N, Kramer K, Götze K, Bassermann F, Schlegl J, Ehrlich HC, Aiche S, Walch A, Greif PA, Schneider S, Felder ER, Ruland J, Médard G, Jeremias I, Spiekermann K, Kuster B (2017) The target landscape of clinical kinase drugs. Science 358 (6367):eaan4368
63. Dart ML, Machleidt T, Jost E, Schwinn MK, Robers MB, Shi C, Kirkland TA, Killoran MP, Wilkinson JM, Hartnett JR, Zimmerman K, Wood KV (2018) Homogeneous assay for target engagement utilizing bioluminescent thermal shift. ACS Med Chem Lett 9(6):546–551
64. Stoddart LA, Vernall AJ, Denman JL, Briddon SJ, Kellam B, Hill SJ (2012) Fragment screening at adenosine-A3 receptors in living cells using a fluorescence-based binding assay. Chem Biol 19(9):1105–1115
65. Dubach JM, Kim E, Yang K, Cuccarese M, Giedt RJ, Meimetis LG, Vinegoni C, Weissleder R (2017) Quantitating drug-target engagement in single cells in vitro and in vivo. Nat Chem Biol 13(2):168–173
66. Goyet E, Bouquier N, Ollendorff V, Perroy J (2016) Fast and high resolution single-cell BRET imaging. Sci Rep 6(1):28231
67. Robers MB, Dart ML, Woodroofe CC, Zimprich CA, Kirkland TA, Machleidt T, Kupcho KR, Levin S, Hartnett JR, Zimmerman K, Niles AL, Ohana RF, Daniels DL, Slater M, Wood MG, Cong M, Cheng YQ, Wood KV (2015) Target engagement and drug residence time can be observed in living cells with BRET. Nat Commun 6:10091
68. Chessum NEA, Sharp SY, Caldwell JJ, Pasqua AE, Wilding B, Colombano G, Collins I, Ozer B, Richards M, Rowlands M, Stubbs M, Burke R, McAndrew PC, Clarke PA, Workman P, Cheeseman MD, Jones K (2018) Demonstrating in-cell target engagement using a pirin protein degradation probe (CCT367766). J Med Chem 61(3):918–933
69. Whitworth C, Farnaby W, Koegl M, Schnitzer R, Steurer S, Ettmayer P, Ciulli A (2018) PO-449 optimisation of an AlphaLISA assay for the characterisation of PROTAC-induced ternary complexes within cell lysates. ESMO Open 3(Suppl 2):A198
70. Riching KM, Mahan S, Corona CR, McDougall M, Vasta JD, Robers MB, Urh M, Daniels DL (2018) Quantitative live-cell kinetic degradation and mechanistic profiling of PROTAC mode of action. ACS Chem Biol 13(9):2758–2770
71. Chung C-I, Zhang Q, Shu X (2018) Dynamic imaging of small molecule induced protein–-protein interactions in living cells with a fluorophore phase transition based approach. Anal Chem 90(24):14287–14293
72. Kaji T, Koga H, Kuroha M, Akimoto T, Hayata K (2020) Characterization of cereblon-dependent targeted protein degrader by visualizing the spatiotemporal ternary complex formation in cells. Sci Rep 10(1):3088
73. Paiva S-L, Crews CM (2019) Targeted protein degradation: elements of PROTAC design. Curr Opin Chem Biol 50:111–119
74. Chu T-T, Gao N, Li Q-Q, Chen P-G, Yang X-F, Chen Y-X, Zhao Y-F, Li Y-M (2016) Specific knockdown of endogenous tau protein by peptide-directed ubiquitin-proteasome degradation. Cell Chem Biol 23(4):453–461
75. Khan S, Zhang X, Lv D, Zhang Q, He Y, Zhang P, Liu X, Thummuri D, Yuan Y, Wiegand JS, Pei J, Zhang W, Sharma A, McCurdy CR, Kuruvilla VM, Baran N, Ferrando AA, Kim YM, Rogojina A, Houghton PJ, Huang G, Hromas R, Konopleva M, Zheng G, Zhou D (2019) A selective BCL-XL PROTAC degrader achieves safe and potent antitumor activity. Nat Med 25 (12):1938–1947. https://doi.org/10.1038/s41591-019-0668-z
76. Ottis P, Toure M, Cromm PM, Ko E, Gustafson JL, Crews CM (2017) Assessing different E3 ligases for small molecule induced protein ubiquitination and degradation. ACS Chem Biol 12(10):2570–2578
77. Kerres N, Steurer S, Schlager S, Bader G, Berger H, Caligiuri M, Dank C, Engen JR, Ettmayer P, Fischerauer B (2017) Chemically induced degradation of the oncogenic

transcription factor BCL6. Cell Rep 20 (12):2860–2875

78. Savitski MM, Zinn N, Faelth-Savitski M, Poeckel D, Gade S, Becher I, Muelbaier M, Wagner AJ, Strohmer K, Werner T, Melchert S, Petretich M, Rutkowska A, Vappiani J, Franken H, Steidel M, Sweetman GM, Gilan O, Lam EYN, Dawson MA, Prinjha RK, Grandi P, Bergamini G, Bantscheff M (2018) Multiplexed proteome dynamics profiling reveals mechanisms controlling protein homeostasis. Cell 173(1):260–274. e25
79. Popow J, Arnhof H, Bader G, Berger H, Ciulli A, Covini D, Dank C, Gmaschitz T, Greb P, Karolyi-Özguer J, Koegl M, McConnell DB, Pearson M, Rieger M, Rinnenthal J, Roessler V, Schrenk A, Spina M, Steurer S, Trainor N, Traxler E, Wieshofer C, Zoephel A, Ettmayer P (2019) Highly selective PTK2 proteolysis targeting chimeras to probe focal adhesion kinase scaffolding functions. J Med Chem 62(5):2508–2520
80. Buckley DL, Raina K, Darricarrere N, Hines J, Gustafson JL, Smith IE, Miah AH, Harling JD, Crews CM (2015) HaloPROTACS: use of small molecule PROTACs to induce degradation of HaloTag fusion proteins. ACS Chem Biol 10(8):1831–1837
81. Tovell H, Testa A, Maniaci C, Zhou H, Prescott AR, Macartney T, Ciulli A, Alessi DR (2019) Rapid and reversible knockdown of endogenously tagged endosomal proteins via an optimized HaloPROTAC degrader. ACS Chem Biol 14(5):882–892
82. Winter GE, Buckley DL, Paulk J, Roberts JM, Souza A, Dhe-Paganon S, Bradner JE (2015) Phthalimide conjugation as a strategy for in vivo target protein degradation. Science 348(6241):1376–1381
83. Sun X, Wang J, Yao X, Zheng W, Mao Y, Lan T, Wang L, Sun Y, Zhang X, Zhao Q, Zhao J, Xiao RP, Zhang X, Ji G, Rao Y (2019) A chemical approach for global protein knockdown from mice to non-human primates. Cell Discov 5:10
84. Mullard A (2019) Arvinas's PROTACs pass first safety and PK analysis. Nat Rev Drug Discov 18(12):895. https://doi.org/10.1038/d41573-019-00188-4
85. Nabet B, Ferguson FM, Seong BKA, Kuljanin M, Leggett AL, Mohardt ML, Robichaud A, Conway AS, Buckley DL, Mancias JD, Bradner JE, Stegmaier L, Gray NS. (2020) Rapid and direct control of target protein levels with VHL-recruiting dTAG molecules bioRxiv 2020.03.13.980946. https://doi.org/10.1101/2020.03.13.980946